May 2014

Structure, paleolimnology and basin history of the East Kivu Graben, Lake Kivu, Rwanda from offshore seismic reflection data

Douglas Alan Wood
Syracuse University

Abstract:

Lake Kivu, located at the topographic high point of the western branch of Africa's Great Rift Valley, is regularly subjected to large-magnitude seismic events, violent volcanic discharges, and possible limnic eruptions which pose substantial geohazards to the ~two million Congolese and Rwandan people living around its basin. Although most of the western branch of Africa's Great Rift Valley is amagmatic, Lake Kivu is bordered to the north and south by two volcanic provinces. Subaqueous springs, charged by the active Virunga Magmatic Complex at the north end of the lake, currently inject gas into the deep- hypolimnion, where it remains in solution at high concentrations. Rapid expulsion of these gases into the atmosphere, possibly induced by seismic, meteorologic, or volcanic events, would be devastating to the local population. To assess the potential danger, it is critical to understand the basin's structure, and the effects of magmatism and climate changes on the lake.

Information about past basin structural, and lake surface elevation changes are preserved in the sediments under the lake; these provide information about the region's tectonic and climatic past. Between 2010 and 2013, Syracuse University's Department of Earth Sciences acquired ~1100 km of marine seismic reflection data and six Kullenberg sediment cores from the eastern basin of the lake. Interpretation of these seismic data show that the eastern basin of Lake Kivu is a half-graben, bounded by east-dipping normal faults. Most subsidence is accommodated at the west side of the basin by slip along two north striking, offset growth faults which are located east of Idjwi and Iwawa Islands. Strain between these faults is accommodated by oblique strike-slip along a northeast striking, transfer fault. Oblique slip along other northeast-striking faults may accommodate extension between more recent, north striking fault

segments. This could account for the irregular shape of Lake Kivu's basin, islands, and shoreline.

The >1.5 km sedimentary section observed in the marine seismic reflection data records extreme climate changes through the late Pleistocene and Holocene. Truncated surfaces indicate that the lake has experienced at least three periods of desiccation. Two of these events correlate to prolonged times of aridity interpreted within the sedimentary records of other African Great Lakes. Between these desiccation periods, the maximum lake surface has varied over a range of >400 m, controlled at different times by climate or the basin's structural configuration. At ~12 ka, there was a transgression from a lowstand of ~370 m below the current lake level, to a level above the current water position. This transgression is reported as induced by a sudden, rapid expansion of the Virunga Volcanic Complex which blocked the northern outlet of the lake, forcing it to a higher, southern spill point through Bukavu Bay; however data presented herein show that it was likely caused by a change in the regional climate. Sediment core data indicate that the transgression occurred over a time span of ~100 years which was likely too short of a period for such a large magmatic expansion. Seismic data show that for most of the lake's past, prior to this -370 m lowstand, the lake level was at ~310 m below the modern lake level, indicating that the lowstand underfilled the lake basin. In this circumstance, the basinal spill point did not control the lake level. Other East African Lakes also transgressed from low stands at approximately the same time, indicating that there was a regional change to wetter climate conditions. Inflation of the Virunga Volcanic Complex, which likely occurred gradually before, or during the lowstand, raised the topographic threshold to the north forcing the lake to spill out of the southern, Bukavu Basin when the transgression occurred.

Structure, paleolimnology and basin history of the East Kivu Graben, Lake Kivu, Rwanda from offshore seismic reflection data

by

Douglas A. Wood

B.A., Hobart College, 2005

Thesis
Submitted in partial fulfillment of the requirements for the degree of
M.S. in Earth Sciences

Syracuse University
May, 2014

Acknowledgements:

I would like to thank my adviser Dr. Christopher A. Scholz, first for inviting me to work in Africa and introducing me to the wonder of the Great Rift Valley Lakes, then for supporting me through my graduate student studies. His is the boundless, driving energy behind what seems an impossible task of assembling, and moving massive amounts of equipment, and expertise into remote locations to collect these data. I also want acknowledge the rest of the Lacustrine Rift Basin Research Program team from Syracuse University's Earth Sciences Department. Technicians Peter Cattaneo and Jacqueline Corbett: Pete for his expertise in the field acquiring the seismic data, and his continuous maintenance and 'helpdesk' support for the complex software needed to process and interpret these data. Jacqueline I want to thank for her work preserving the core collection and being the most organized person in the field. I would like to thank my colleagues and fellow graduate students Mattie Friday, Stoney Gan, Tannis McCartney, Amy Morrissey, and Xuewei Zhang for support, encouragement, and edits. Xuewei deserves a specific acknowledgement along with Robert Hecky from the Large Lakes Observatory, University of Minnesota, Duluth for their work on the radiometric ages included in this work. I would also like to thank members of my defense committee: Cynthia J. Ebinger from the University of Rochester and Christopher Junium, Christopher A. Scholz, and Bruce H. Wilkinson from Syracuse University.

For field work in the Republic of Rwanda we thank the government of Rwanda for permission to conduct this research. We are grateful for the assistance in the field by Irénéé Nizere from the Rwanda Ministry of Natural Resources, Joseph Katarebe and colleagues from Kivuwatt. Ltd., and the Kigali Institute of Science and Technology for facilitating our field efforts. Other contributors and collaborators in the field include Robert Hecky from the

University of Minnesota, Cynthia Ebinger from University of Rochester, Anthony Vodacek from Rochester Institute of Technology and especially our crew in Kibuye including Elie Kabende and our driver and guide Victor Rugambage. I would like to thank Capt Jack Greenberg for his safe and productive operation and management of our vessels and crew. We also thank those organizations which supported this work financially including The MacArthur Foundation, Vanoil Energy, Ltd., BP, Chevron, Shell, Petrobras and Cobalt. There are countless others to thank, too many to name who have been involved in supporting this work.

Finally, I would like to thank Catherine Galloüet for her patience with me throughout this process.

Table of contents:

Figures and Tables:

Introduction:

The tectonic uplift and extension which led to formation of the East African Rift (EAR) altered the landscape, redirected drainage patterns, created new ecological corridors and changed regional climate, all of which influenced the long term evolution of the flora and fauna of the continent (Roberts et al., 2012). The rising mantle plume which is responsible for this uplift and subsequent rifting is deflected by the relatively thick, cold Tanzanian Craton, to break the continental crust along the separate eastern (Kenyan) and western branches of the EAR (Ebinger and Sleep, 1998; Ebinger and Furman, 2002). Rifting probably follows former zones of weakness, such as Proterozoic mobile belts (e.g., Nyblade and Brazier, 2002, Roberts et al., 2012). The eastern branch exhibits widespread volcanism whereas the western branch has only four localized magmatic provinces along its ~2500 km length (Nyblade and Brazier, 2002; Ebinger and Furman, 2002), but it is much more seismically active (e.g., Wong and von Herzen, 1974; d'Oreye et al., 2011). Two of the four volcanic regions of the western branch, the South Kivu and Virunga magmatic provinces, are located at the south and north ends of Lake Kivu. Both of these regions are currently seismically active, and the Virunga complex contains the most active volcano in the continent (Smets et al., 2010).

As the western branch of the EAR is overwhelmingly amagmatic, the basins formed by extension are inclined to fill with deep lakes rather than thick volcanic, or volcaniclastic packages (Tiercelin and Lezzar, 2004). About 1680 km of the length western branch is covered by lakes, more than ~67 percent of its overall length, whereas less than 25 percent of the eastern branch is covered by water. Because of the abundance of deep water strata, the geologic history of the western rift may be well-recorded in the lake systems. Two important controls on lithofacies are climate and tectonic subsidence (Bally, 1988), so by examining sedimentary

strata, climate history and the effect of tectonics on the basin may be interpreted. This study applies remote sensing methods, utilizing marine seismic reflection techniques, and combines these with direct observations of lake core samples from the eastern basin of the lake in order to interpret and map structural deformation, estimate the amount of tectonic extension, further constrain the dynamic lake level variations and estimate the minimum age of the eastern basin of Lake Kivu.

Geologic Background:

Lake Kivu is a deep, permanently stratified lake, and at 1463 m above mean sea level, is the highest of Africa's Great Lakes (Degens et al., 1973). It has a surface area of ~2,060 km^2, a catchment area of ~7,140 km^2 and reaches a maximum depth in its northern basin of ~485 meters (Stoffers and Hecky, 1978) (Fig. 1). The lake is situated on the border between the Democratic Republic of the Congo (DRC) and the Republic of Rwanda. Lakes in temperate or high latitudes tend to seasonally mix their water columns from top to bottom when surface waters are exposed to cold winter weather conditions. Cooling surface water parcels thermally contract, increasing in density until they sink, leading to lake mixing. Many deep tropical lakes, however, unexposed to cold winter conditions, tend to be perpetually stratified. A deep tropical lake generally stratifies into a meromictic state, with an upper, epilimnic layer, made less dense by warming from solar insolation and subsequent thermal expansion. This epilimnic layer floats above a relatively dense, hypolimnic layer which generally becomes anoxic due to isolation from the atmosphere (Spigel and Coulter, 1996; Crowe et al., 2008).

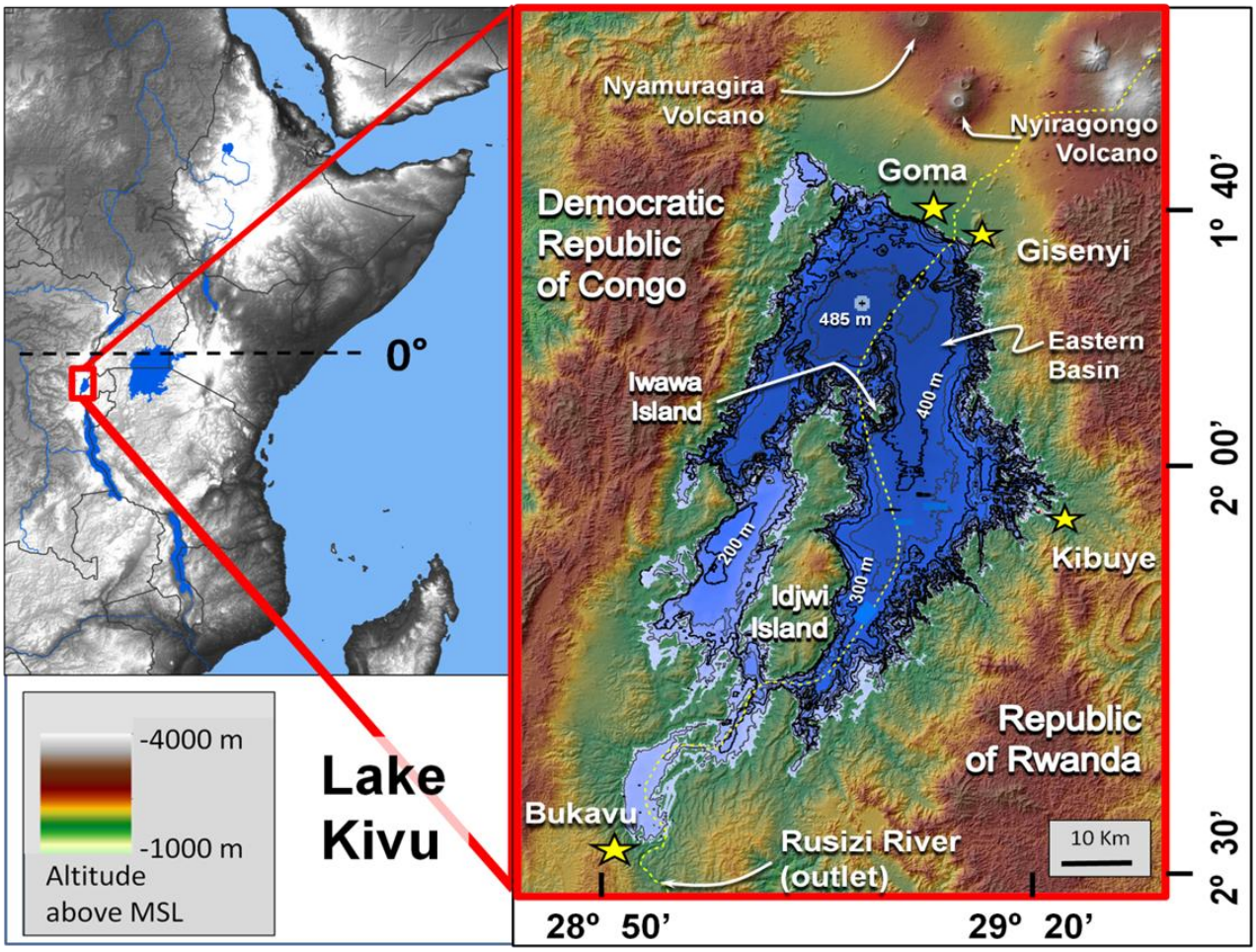

Figure 1. Study area, Lake Kivu, Rwanda, in the western branch of the Great Rift Valley. Bathymetric contour interval = 50 m. Stars represent major cities, yellow dashed line = international border.

Lake Kivu is an unusual meromictic lake in that bottom waters are warmer than the epilimnion by as much as ~1.5º C (Spigel and Coulter, 1996). Stable density stratification is maintained by a high concentration of solutes in the hypolimnion, making bottom water as much as 4.5 g/l more dense than the surface water (Bhattarai et al., 2012). Seasonal mixing within the epilimnion of the lake reaches a depth of 50 to 80 meters (Schmid et al., 2005); below this depth, an estimated 250 km^3 of CO_2 and 55 km^3 of methane, at STP, are in solution in the hypolimnion (Tietze, 2000). These high concentrations of dissolved gases are due to the influx of CO_2 into the lake's deep water via magmatically-charged springs and its subsequent methanogenesis by

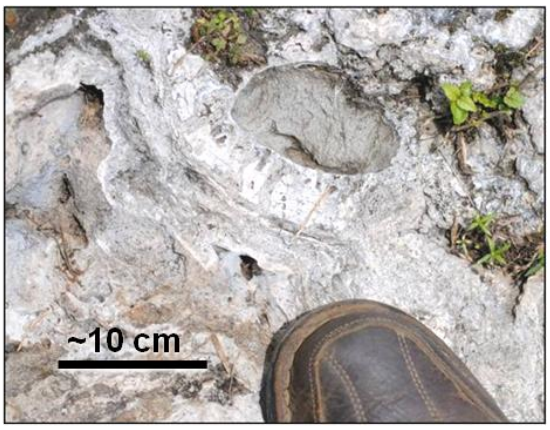

Figure 2. Carbonate tufa encrusting bedrock cobbles, Lake Kivu shoreline, Kibuye, Rwanda, 2012.

benthic microorganisms (Bhattarai et al., 2012). Every liter of Kivu water deeper than 250 m contains 1.5 liters of CO_2, at STP, in solution (Kempe and Degens, 1985). These dissolved gases present a potential geohazard to the people living near the lake, due to the possibility of overturn and rapid release into the atmosphere; such limnic eruptions have occurred in the smaller Lakes Monoun and Nyos, Cameroon in 1984 and 1986 respectively, killing more than 1700 people by asphyxiation (Kling, et al., 1987). The current limited biological diversity of the lake, and evidence from the lake's sediment over the past 5000 years suggest that Lake Kivu turnover events have occurred in the past (Haberyan and Hecky, 1987). A small methane extraction plant is currently in operation at the north end of the lake offshore of the city of Gisenyi, and a much larger facility is under construction near Kibuye (Fig. 1). These plants are intended to extract methane and CO_2 from the hypolimnic waters, vent the CO_2 into the atmosphere in order to alleviate the risk of limnic eruption, and exploit the methane to provide up to 100 Mw of electricity to the region (Environmental and Social Impact Assessment Summary, Kivuwatt Power Project, 2010).

Lake Kivu is chemically bimodal, with acidic hypolimnic waters (pH of ~6), a result of the high concentration of dissolved CO_2, whereas the epilimnion is alkaline (pH of ~9), where waters mix with the atmosphere and excessive CO_2 is ventilated (Bhattarai, et al., 2012). Carbonates precipitate in the shallows and along the lake's shore (Fig. 2), but the modern deep waters are corrosive to carbonates preventing deposition (Degens et al., 1973). Ancient deep

lake sediments contain alternating bands of siliciclastic, and carbonate-rich sediments (Stoffers and Hecky, 1978), indicative of substantial historic variations in the benthic conditions. This variation might be due to dynamic lake level changes or excursions from stratified conditions.

Lake Kivu drains southward from the Bukavu Basin, down the Rusizi River ~100 km into Lake Tanganyika (Figs. 1, 3). Kivu is a major contributor of water, and the primary contributor of Virunga-derived solutes into Tanganyika (Stoffers and Hecky, 1978). Currently the Kivu-based inflow into Lake Tanganyika via the Rusizi River exceeds Tanganyika's outflow via the Lukuga River; termination of Kivu's outflow into the Rusizi River would close Lake Tanganyika and lower its surface by ~75 meters if other factors remain constant (Haberyan and Hecky, 1987).

The western branch of the EAR is formed by a chain of generally north-south oriented, ~100 km long asymmetrical border fault systems with throws of 1-6 km (Ebinger, 1989a). The largest lake basins, such as Tanganyika's are a series of these fault systems crosscut by accommodation zones; these accommodation zones include relay ramps and structures transverse to the rifts (Ebinger, 1989b). The Kivu Rift is a single-segment system with the primary border faults located on the western side of the basin, with a basement horst, Idjwi Island, separating the western (northern) and

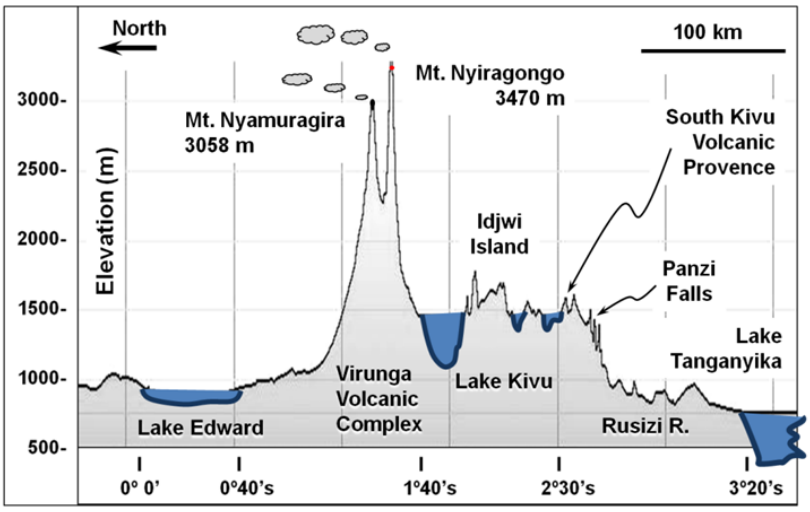

Figure 3. Topographic profile of the Western Branch of Africa's Great Rift Valley from Lake Edward to the north end of Lake Tanganyika. Topography from *Google Earth*, 2013.

eastern grabens (Fig. 1) (Ebinger, 1989a). It appears that magmatism around the Kivu basin began in the Miocene and proceeded from north to south, with the oldest extrusive, tholeiitic basalts from the Virunga Province dated by $^{40}K/^{40}Ar$ at ~ 11 Ma (Kampunzu et al., 1998), and the oldest tholeiites from the South Kivu Province dated at ~10 Ma (Pasteels et al., 1989). A change toward alkaline basalts, which signal mantle lithosphere derived melts occurred at ~8.9 Ma in the Virunga area, and ~7.5 to 6 Ma in the South Kivu Province (Pasteels et al., 1989; Kampunzu et al., 1998). More recent studies of dated sediments and paleodrainage patterns in the Rukwa Rift, south of the Kivu rift, however, show that the onset of extension in that part of the western branch of the EAR may be 26-24 Myr ago (Roberts et al., 2012). Constraining the age and sequence of rifting events in the EAR remains controversial.

Lake Kivu reportedly drained northward, to Lake Edward, and was a source of the White Nile prior to northern impoundment by the growth of Virunga volcanics (e.g., Brooks, 1950; Degens et al., 1973; Haberyan and Hecky, 1987). Supporting this hypothesis, lake fauna, although limited in number of species, are similar to the taxa of Lake Edward to the north but are unrelated to those in Tanganyika (Beadle, 1981); an exception is the invasive Tanganyika Sardine (*Limnothrissa miodon*), locally referred to as sambaza, which was successfully introduced into Lake Kivu in 1963 in order to create a commercial fishery (Beadle, 1981). Also, Virunga-derived solutes are not observed in Lake Tanganyika sediments before 10.6 ka suggesting that prior to that time Lake Kivu did not drain to Lake Tanganyika (Felton et al., 2007). Earlier data show that the range of Kivu lake level change exceeds 400 meters; paleobeach deposits were recovered from cores at ~300 meters water depth (Stoffers and Hecky, 1978), and diatomaceous strata are observed on Idjwi Island ~120 meters above the modern lake (Degens et al., 1973). Estimates of the timing of this specific, >400 meter transgression place it

in the early Holocene from ~10,000 ybp (Stoffers and Hecky, 1978), to the late Pleistocene ~12,400 ybp (Olson and Broecker, 1959).

Methods:

Between 2010 and 2013, Syracuse University's Department of Earth Sciences acquired over 1100 km of marine seismic reflection data, and 25 Kullenberg sediment cores from the eastern basin of Lake Kivu. Data were acquired in Rwandan territorial waters from a 24-foot a rigid inflatable boat (RIB) and the 40-foot, twin hulled *R/V Kilindi* (Figs. 4, 5); both vessels are owned by Syracuse University. Positioning for each vessel was acquired by a Trimble™ AG132 GPS receiver. During airgun-sourced seismic operations, differential GPS data were corrected to sub-meter accuracy using the Omnistar™ system.

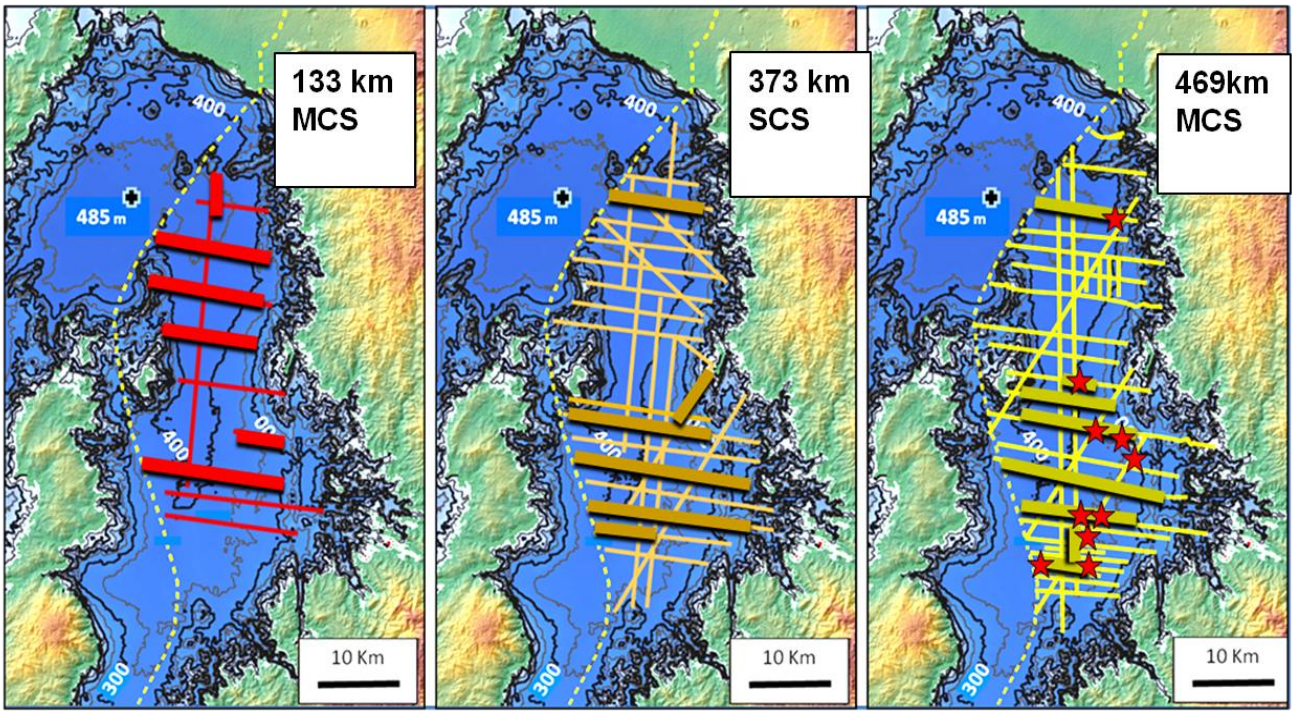

Figure 4. Multi-channel seismic (MCS), single-channel seismic (SCS), and CHIRP sonar data acquired from Rwandan territorial waters in the eastern basin of Lake Kivu. Highlighted lines are presented in this study. Stars in right most map are approximate locations of the ten sediment cores described or sampled for this study.

Figure 5. Syracuse University research vessels: *R/V Kilindi* and rigid inflatable boat (RIB) near Kibuye, Rwanda.

Different reflection seismic configurations and acoustic sources result in different data resolution and sediment penetration characteristics. Lower power acoustic sources using higher frequency transducers image the sub-surface at higher resolution, but the signal is attenuated within a short distance below the sediment-water interface. More powerful and lower-frequency seismic sources penetrate farther into the sediment, but cannot resolve small scale sedimentary features as effectively. Use of a long, multi-channel seismic streamer is problematic near shorelines and international borders resulting in shorter seismic profiles. Three different reflection seismic systems were used over the East Kivu Graben and are presented in this study: low-frequency, multi-channel reflection seismic (MCS) to attain the maximum sediment penetration and observe the overall basin structure: single-channel reflection seismic (SCS) for moderate penetration and detail: and high frequency CHIRP for decimeter scale resolution of the uppermost sediments. Table 1 shows characteristics of each acquisition system used on Lake Kivu.

The 600 m (MCS) streamer towed by the *R/V Kilindi*, contained 48 hydrophone groups spaced 12.5 m apart, and was towed with a 60 m lead-in cable. The streamer was maintained at a depth of 5 meters by three Digicourse^{TM} cable-levelers (birds). The MCS and single-channel seismic (SCS) acoustic source was an ION^{TM} 40 in^3 sleeve gun charged to 2000 psi and towed 16

m aft of the vessel and 2.5-3 m below the water surface. The average acquisition speed was ~4-5 kts and the shooting interval was 12.5 m.

Table 1. Seismic reflection data acquisition parameters.

Marine reflection seismic type	total km acquired	source	data bandwidth	receiver	acquisition system	recording length	max Kivu sediment penetration
Multi-channel (MCS)	133 km	ION 40 cu-in	5-250 Hz	ITI, 600 m 48 channel, 12.5m group interval	OYO 24 bit DAS-1, 48 chan	4000 ms	> 1500 m
Single-channel (SCS)	373 km	ION 40 cu-in Bolt 10 cu-in	50 Hz - 1 kHz	Benthos 12 Teledyne hydrophone streamer	Geoacoustics analog rcvr, Chesapeake software	2000 ms	~150 m
CHIRP	469 km	Edgetech SB-424	4-16 kHz	Edgetech SB-424	Edgetech Discover 3100 software	variable	~25 m

The MCS data were processed at Syracuse University using *Promax 2D*™ software by Landmark Graphics, Corp. Commercial processing was also completed by Statcom, Ltd., Calgary, Alberta, Canada. MCS data were bypassed filtered between 5 Hz and 250 Hz, and Kirchoff time migrated prior to common depth point (CDP) stacking; F-X deconvolution was applied afterward. Interpretation was conducted at Syracuse using *DecisionSpace*™, version 5000, by Landmark Graphics, Corp. The MCS data presented in this study are converted from two-way travel time (TWTT) to depth below current lake surface by applying the internal velocity picks created for each line.

A total of 373 km of SCS data were acquired using a Benthos™ streamer with 12 Teledyne™ hydrophones (table 1). The acoustic source used was an ION™ 40 in^3 sleeve gun when being acquired concurrently with MCS, otherwise, the source was a Bolt™ 10 in^3 air gun; both pneumatic acoustic sources were charged to 2000 psi and triggered every 12.5 meters. The 2000 ms SCS data were conditioned by a Geoacoustics ™ analog receiver, and recorded by

Chesapeake™ , Sonarwiz software on a PC computer. SCS data were processed using Promax 2D ™, and bandpass filtered between 50-1000 Hz. SCS interpretation was also conducted with DecisionSpace ™ software at Syracuse University.

The acoustic source and acquisition device for the ~469 km of high frequency CHIRP data was an Edgetech™ SB-424 towfish towed ~1-1.5 meters below the lake surface from the 24 foot RIB. The CHIRP data were received through an Edgetech 3100p deck unit, and match filtered between 4 and 16 kHz. CHIRP data were recorded and processed using Edgetech Discover 3100™ software. The pulse frequency and recording length for CHIRP profiles vary with water depth and sediment penetration. SCS and CHIRP profiles are presented with TWTT in milliseconds (ms) on the vertical axis. For convenience, a scale is included on the left which displays the estimated depth below the current lake level in meters on all figures. Conversion from TWTT to meters for SCS and CHIRP profiles assumes a water column and upper sediment sound speed of 1500 m/s. This sound speed value is calculated based on an average water column temperature of 23º C and a salinity of 5 g/l (Bhattarai et al., 2012). About 127 km of 1 kHz, digital Boomer reflection data were also acquired; these are not presented in this study.

At total of 25 sediment cores were acquired aboard the *R/V Kilindi* using a Kullenberg piston coring system in January of 2012, and March of 2013; ten of these cores are sampled or described here (Fig. 4). Sediments were collected in 7 cm diameter polycarbonate tubes with a driving weight of 840 pounds (380 kg); the maximum recovery was ~9 m. The cores were delivered to the National Lacustrine Core Repository (LaCore) at the University of Minnesota where they were scanned for density and magnetic susceptibility, split, sub-sampled, and imaged. Plant samples for radiometric dating by ^{14}C were removed from cores then processed by Beta

Analytic, Miami, Florida. The resulting radiocarbon ages were calibrated using the CalPal-2007 [online] (Danzeblocke et al., 2013) then correlated stratigraphically to core KIVU12-19A (Table 2).

Depths presented in this study are reported in meters relative to the modern lake level (MLL) datum which is the height of the lake surface during this study. The lake surface is assumed to be at an altitude of 1465 meters above sea level.

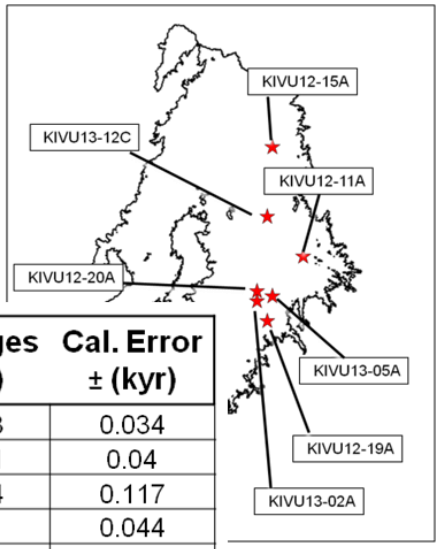

Table 2. Locations and radiometric ages of terrigenous macrofossils collected from seven cores. These were dated by ^{14}C then correlated to core KIVU12-19A. Map shows the approximate recovery location for each of these sediment cores.

Sample Number	Core	Downcore Depth (cm) *	Coventional Ages (yr)	Error ± (yr)	Cal. Ages (kyr)	Cal. Error ± (kyr)
1	KIVU12-11A	222	1110	30	1.018	0.034
2	KIVU12-19A	370	3390	30	3.641	0.04
3	KIVU12-19A	412	4440	30	5.104	0.117
4	KIVU12-19A	514	5960	30	6.8	0.044
5	KIVU12-19A	563	6270	40	7.212	0.036
6	KIVU12-19A	636	7430	40	8.265	0.052
7	KIVU12-19A	653	8100	40	9.051	0.04
8	KIVU13-12C	472	5270	40	6.068	0.084
9	KIVU13-12C	614	7060	40	7.9	0.038
10	KIVU13-15A	607	6670	40	7.545	0.032
11	KIVU13-15A	640	7210	40	8.044	0.057
12	KIVU13-02A	709	8390	40	9.408	0.059
13	KIVU13-20A	296	2140	30	2.172	0.095
14	KIVU13-20A	774	9100	50	10.284	0.054
15	KIVU13-05A	794	10000	40	11.496	0.142

* Downcore depths are stratigraphically correlated to core KIVU12-19A

Results: Basin Structure

Marine multichannel seismic (MCS) reflection profile MCS-22 shows the eastern basin of the lake to be a wedge-shaped package of sediments and a system of east dipping synthetic normal faults (Fig. 6). MCS acoustic penetration reaches a depth of ~1500 meters below the lake floor near the west side of this profile. The westernmost, East Iwawa Fault (EIF) exhibits the greatest throw in this profile. This is a listric fault which dips eastward at ~50º near the lake bed then dip shallows to ~40º ~1500 m down section. The EIF fault is observed in MCS profiles 14, 22, and 18 (Figs. 6, 7a, b). The EIF, however, is not observed in line MCS-36 which crosses the basin to the south of the other MCS lines (Fig. 7c). Overall, the data show the basin structure to be a north-striking, half-graben with a west dipping hanging wall (Fig. 8). The MCS data show that the hanging wall has a dip of ~11º in the north of the basin (Fig. 7a). The hanging wall dip angle decreases to the south to ~6º at line MCS-36 which is south of Iwawa Island (Fig. 7c). The relatively steep-dipping, half-graben structure of the eastern basin accommodates a narrow band of thick sediments to the east of Iwawa Island (Figs. 9-12). South of Iwawa Island, where the footwall dips less steeply toward Idjwi Island, the sediment wedge is wider (Fig. 9).

In the northern part of the basin, higher resolution Single Channel Seismic (SCS) data exhibit some small scale, west-dipping faults that are antithetic to the east dipping faults (Fig. 13b). These small scale faults show sediment displacements of less than ~25 meters. Antithetic faults are not observed in the southern part of the basin. Three northeast striking faults are interpreted from MCS data at the north end of the study area (Fig. 8). These faults show displacement of deeper sediments but little recent activity. These faults are subparallel to a northeast striking, oblique transfer fault south of Iwawa Island (Fig. 8) which is interpreted from bathymetry (Zal. 2013).

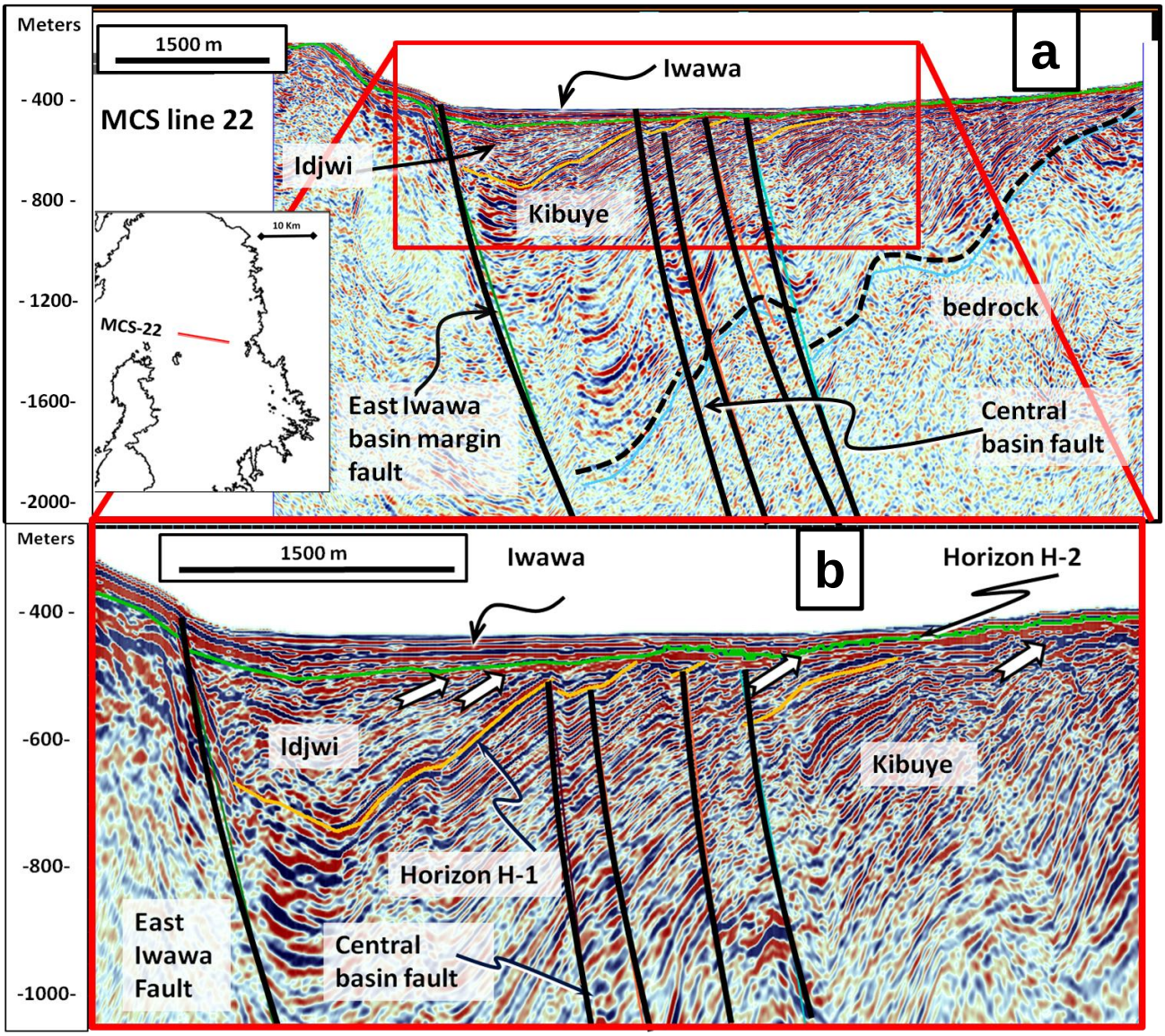

Figure 6. Multichannel profile MCS-22 north-east of Iwawa Island (a). Expanded view of line MCS-22 (b). Vertical scale = meters below modern lake surface. Profile shows a half-graben formed by east dipping faults. There is up to ~1500 meters of sediment section in three major named sedimentary sequences: Kibuye, Idjwi, and Iwawa, separated by two truncation surfaces: H-1 and H-2. White arrows show Idjwi and Kibuye Sequence sediment truncation at the H-2 surface.

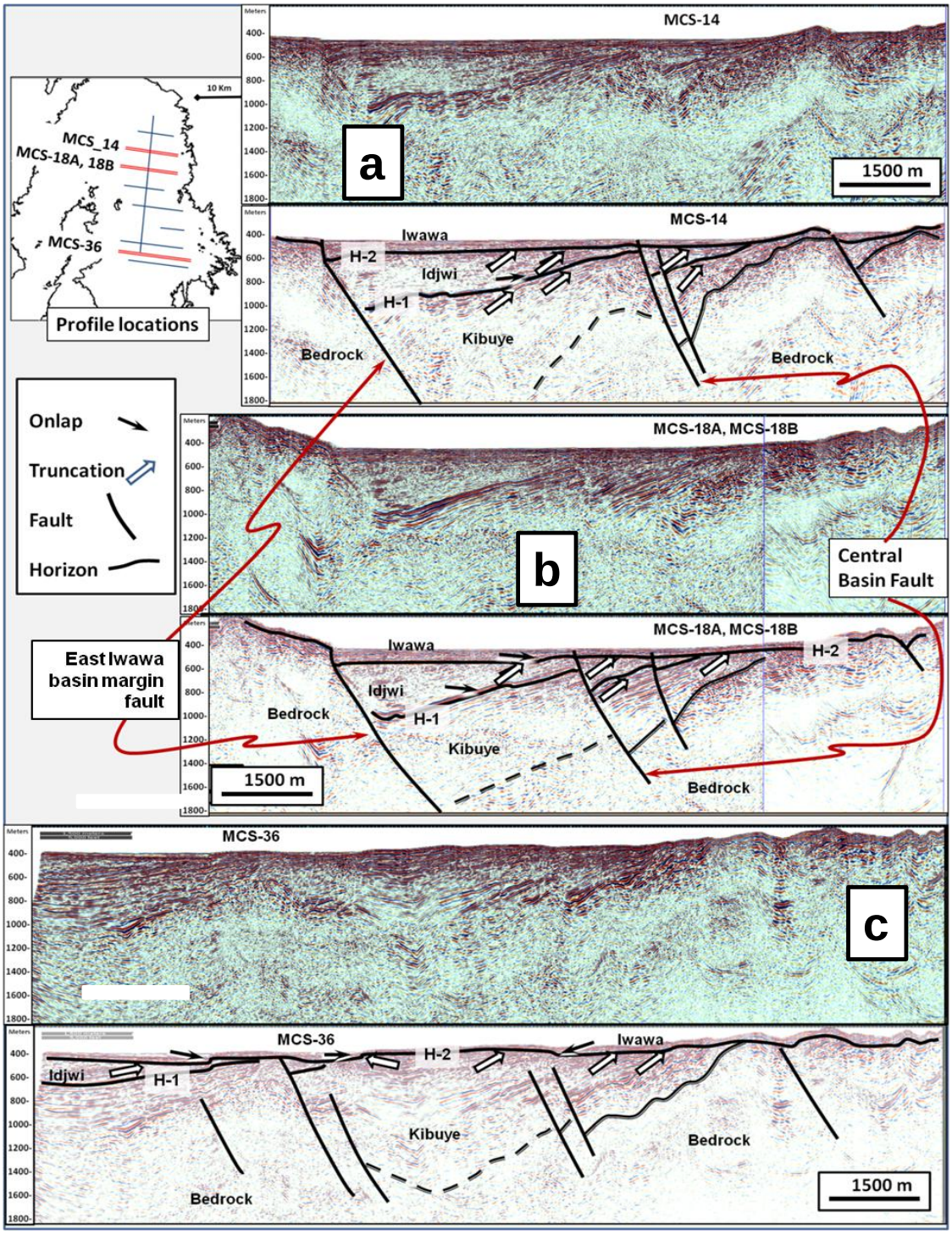

Figure 7. MCS lines 14 (a), 18 (b), and 34 (c) from north to south along survey area, see inset map. Vertical scale is meters below modern lake level. Most tectonic subsidence in the two northern lines is accommodated by the East Iwawa Fault on the west side of the profiles. Line 34 is south of the East Iwawa Fault. Bathymetric high on the west side of line 18 is the northern extension of the crystalline Idjwi Island Horst. Vertical exaggeration ~2x.

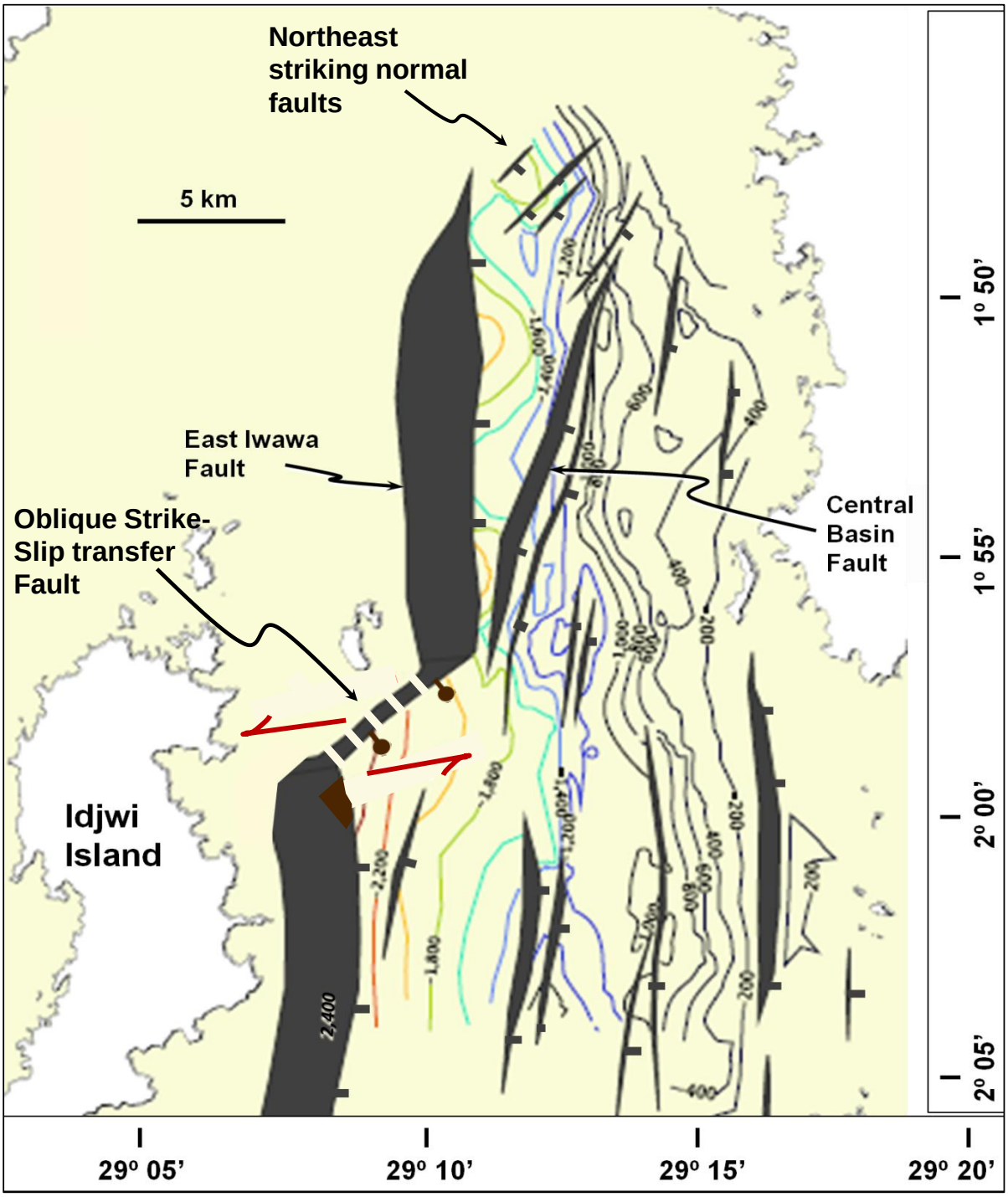

Figure 8. Basement structural contour map of Lake Kivu's eastern basin interpreted from seismic reflection data. Faults south and west of Iwawa Island, and bordering Idjwi Island interpreted from bathymetry (Zal, 2013). Basement depth = meters below modern lake level (MLL), 200 m contour interval. Dark polygons are fault planes, red arrows show relative direction of block movement along left-lateral, oblique transfer fault. Note that the three northern-most faults strike to the northeast, sub-parallel to the transfer

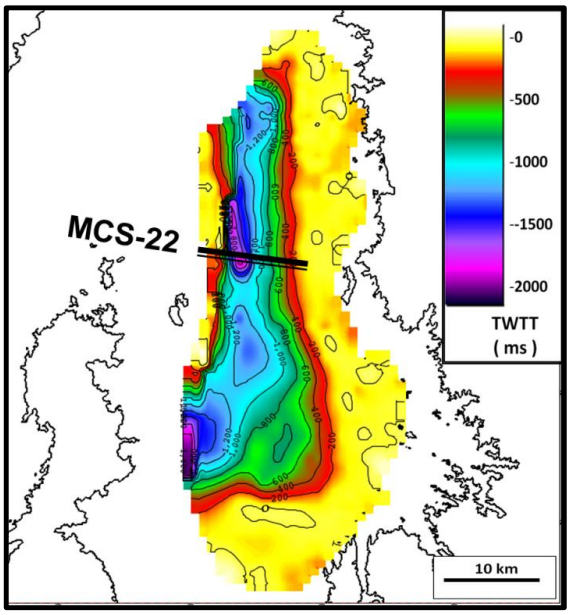

Figure 9. Isochron map showing total sediment thickness. Scale = two way travel time (TWTT) in ms; isochron interval = 200 ms. Maximum sediment thickness is northeast, and south of Iwawa Island.

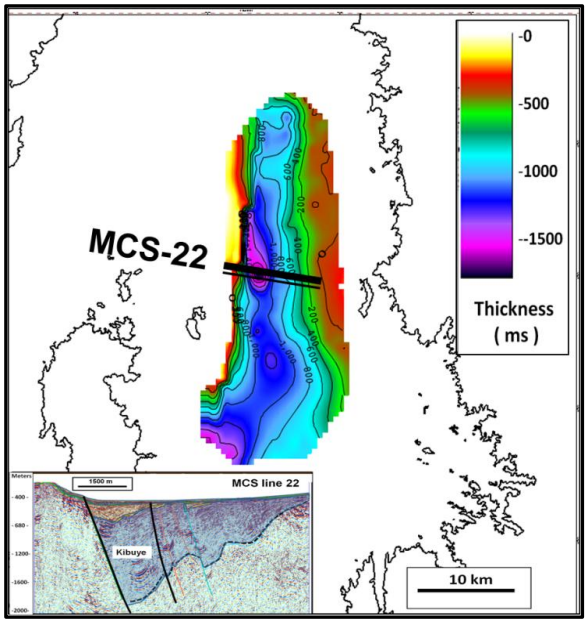

Figure 10. Isochron map of the Kibuye sedimentary sequence which contains most of the sedimentary record. Note that the thickest observed sediments are northeast of Iwawa Island and at the southwest corner of the survey area. Isochron contour interval = 200 ms.

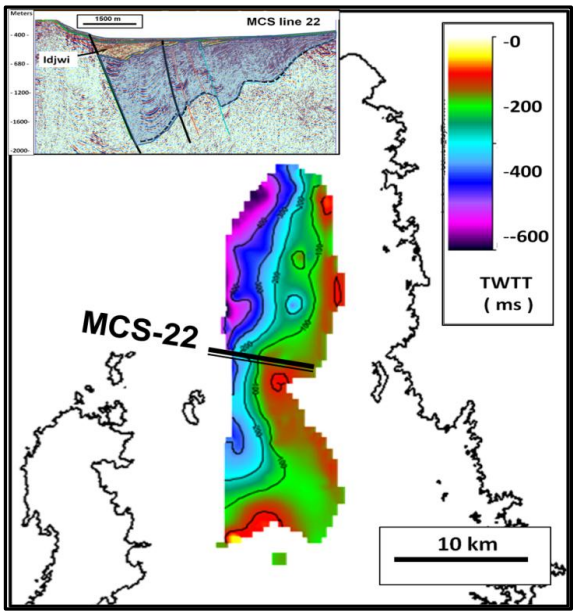

Figure 11. Isochron map of the Idjwi sediment sequence. Note that the thickest Idjwi sediments observed, 600 ms (~450 m), are in the northwest corner of the survey area. Isochron contours = 100 ms.

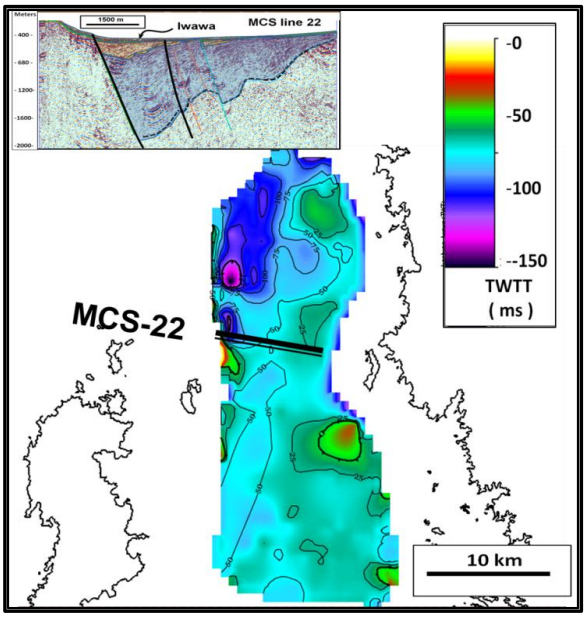

Figure 12. Isochron map of the Iwawa sedimentary sequence which contains the Iwawa-a, Iwawa-b, and Iwawa-c Sequences. Maximum observed sequence thickness is ~150 ms (~100 m) near the northwest corner of the survey area. Isochron contour interval = 25 ms.

Results: Stratigraphy

The north-south striking wedge-shaped sedimentary section shown in MCS lines 14, 18, 22, and 36 reaches a maximum thickness of ~1500 m at the west side of the basin (Figs. 6, 7). The sediment column is divided into three major sedimentary sequences separated by surfaces H-1 and H-2; each of these surfaces is defined by truncation of sediments beneath it (Figs. 6, 7). The lowest, and thickest of the sedimentary packages is the Kibuye Sequence which rests above the bedrock. It is ~1200 m thick northeast of Iwawa Island at the point of maximum throw of the East Iwawa Fault (Fig, 10). The top of the Kibuye Sequence is truncated by surface H-1 (Figs. 6, 7). Above the Kibuye Sequence, and onlapping the H-1 surface, is the Idjwi Sequence section (Fig. 11); this sequence reaches a maximum thickness of ~450 meters in the north-west of the study area (Fig. 11). Surface H-2 shows extensive truncation of both Idjwi and Kibuye Sequence sediments (Fig. 6).

In the southern part of the basin, the H-2 surface follows channel-like incisions cut into Idjwi and Kibuye Sequence sediments (Figs. 14b, 15a,b). The uppermost major sedimentary sequence observed in the MCS data, the Iwawa Sequence, onlaps the H-2 truncation surface, and reaches a thickness of ~100 meters in the northwestern corner of the survey area (Fig. 12). Kibuye Sequence sediments tend to be thickest toward the southwest and west-central parts of the basin (Fig. 10), whereas the upper, Idjwi and Iwawa sediments are observed to be thickest near the northwest corner of the survey area (Figs. 11, 12).

The higher frequency SCS and CHIRP seismic acquisition systems resolve three sub-sequences that comprise the Iwawa Sedimentary Sequence, and are below the resolution of the MCS data. Coincident seismic profiles MCS-10, SCS-10 and CHIRP KIVU12-026 (Fig. 13),

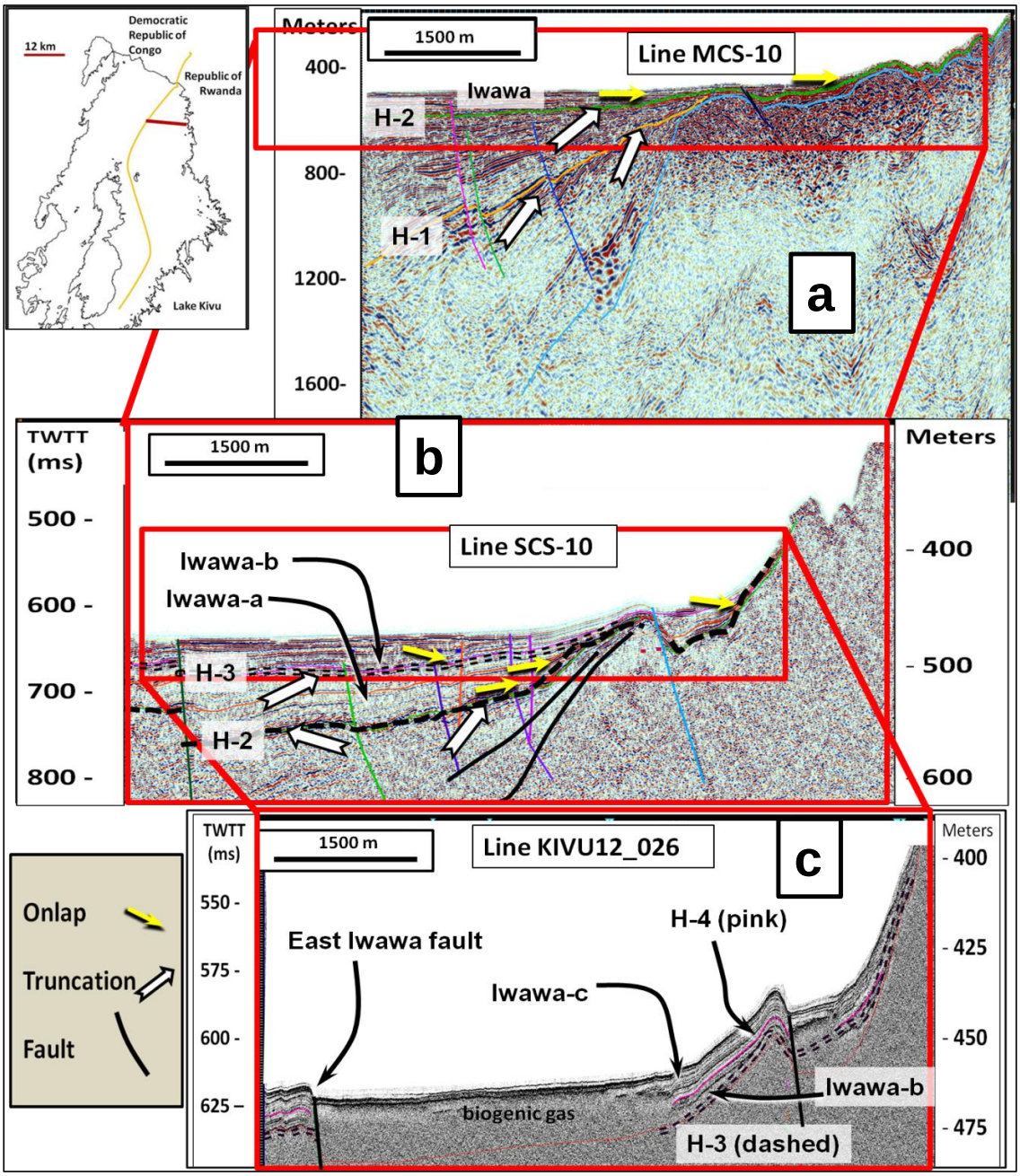

Figure 13. Coincident multi-channel line MCS-10 (a), single channel line SCS-10 (b), and CHIRP line KIVU12-026 (c), showing characteristic sediment penetration and resolution of each data vintage. Note expanded vertical scale with each successive profile. Single dashed line shown in the SCS profile is surface H-2, which is beyond the penetration of CHIRP. Double dashed line, the acoustic basement of the CHIRP, is the H-3 horizon. The H-4 high –amplitude reflection is a reflective ash layer deposited near the end of the Iwawa-c lake lowstand period. The SCS profile shows small scale, west-dipping antithetic faults which are below the resolution of the MCS data.

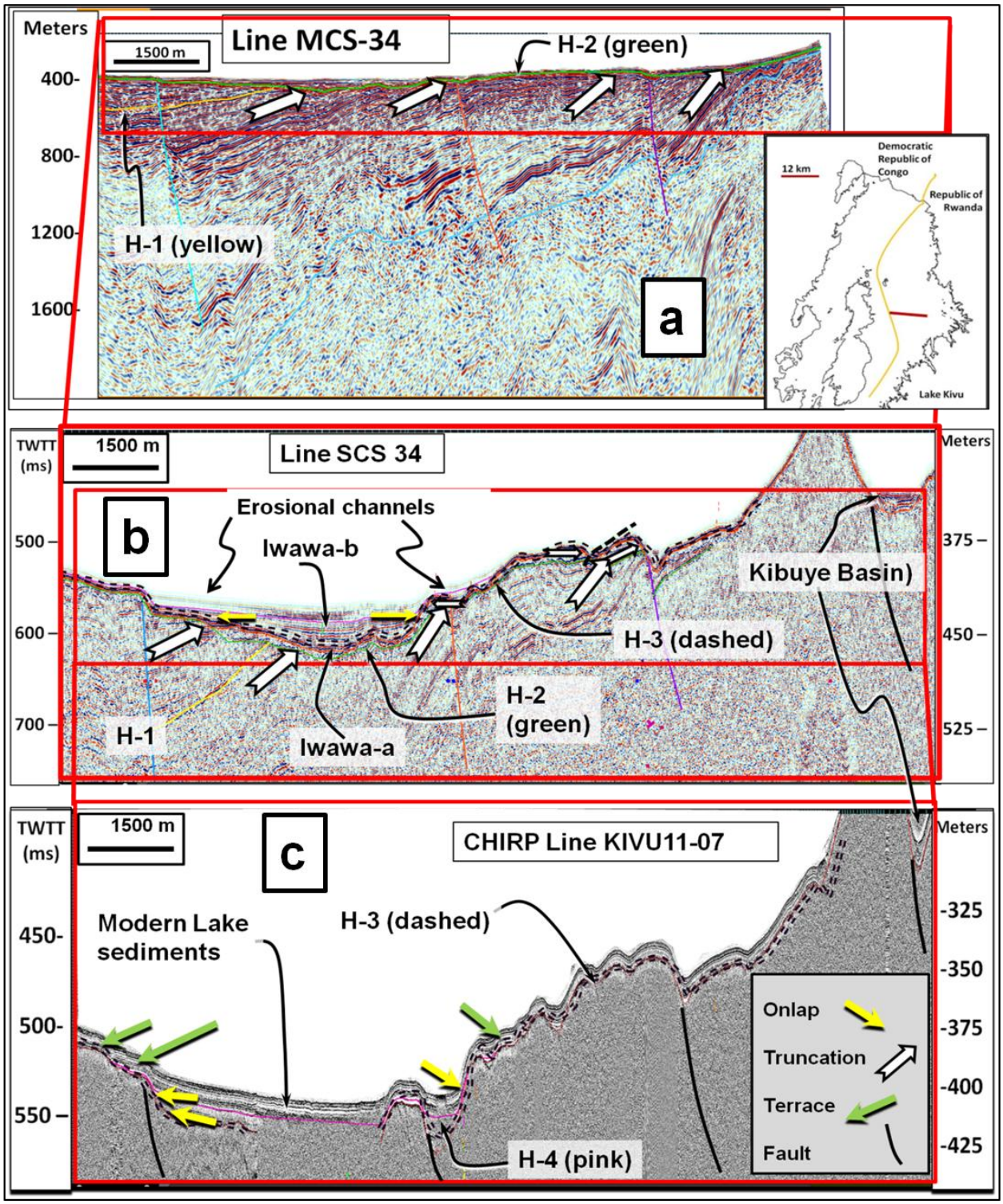

Figure 14. Multichannel line MCS-34 (a), inset shows profile location of coincident single-channel line SCS-34 (b), and inset shows location of profile CHIRP line KIVU12_C_07 (c) sup-parallel and ~1 km to the north. Note erosional channels and benches incised into the Idjwi and Iwawa-a sediments. Kibuye Basin, offshore of the village of Kibuye, is shown on east side of the SCS and CHIRP profiles.

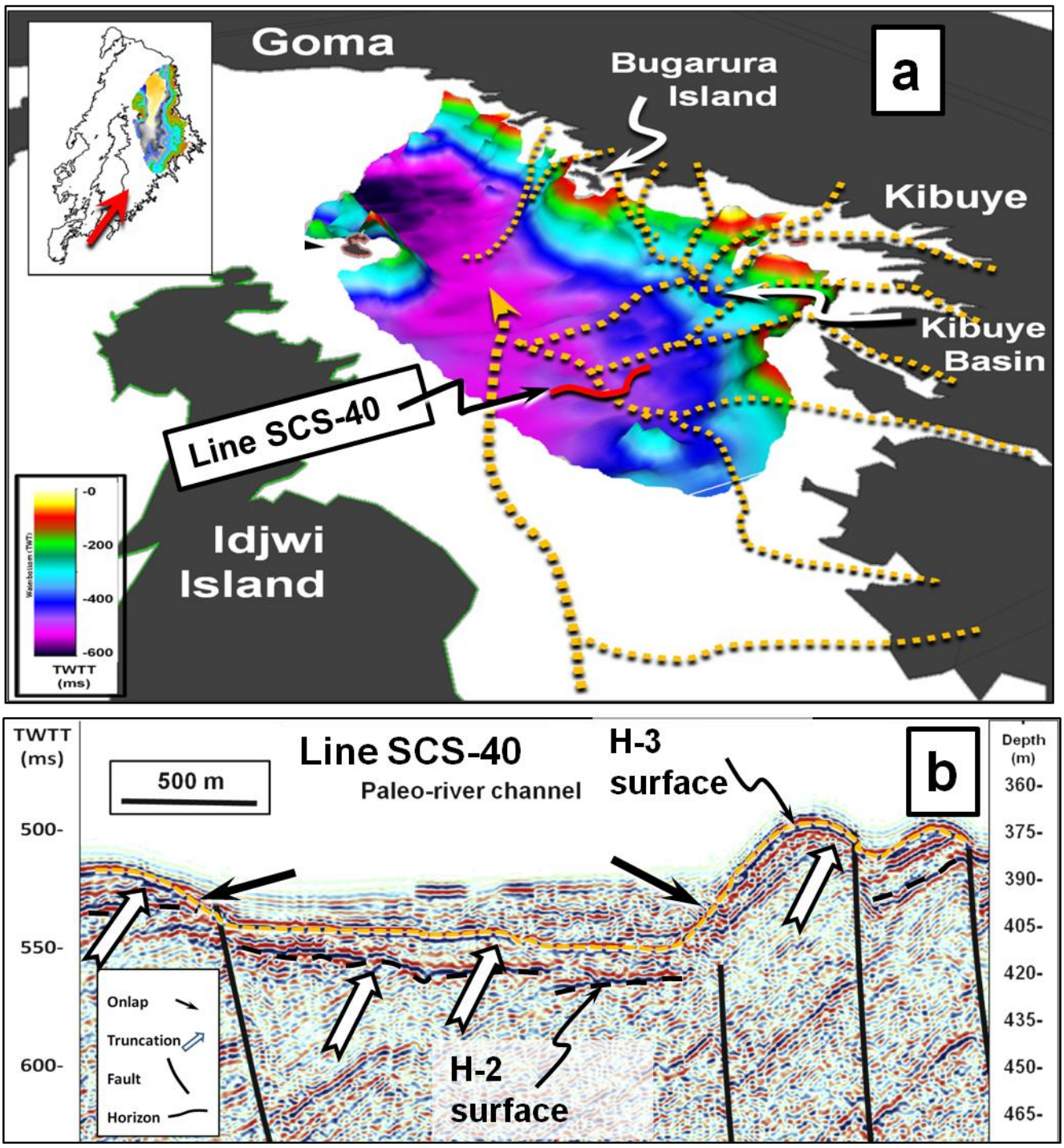

Figure 15. Oblique perspective view of the bathymetry of the eastern basin (a). Dashed lines show the paths of erosional channels incised into lake sediments, red arrow on inset map shows direction of view. Profile SCS-40 (b) shows erosional channel profile incised into lakebed sediments. Currently these channels serve as conduits for deep water density flows. Note: channels conflate in Kibuye Basin (east side, a) then pass through a cut in the western wall of the basin.

acquired near the northern end of the study area expose these sequences. The CHIRP seismic data is attenuated at the H-3 truncation surface (Fig. 13c); the SCS seismic data penetrate surface H-3, but are nearly completely attenuated at the deeper H-2 truncation surface (Fig. 13b). Surface H-2 (Fig. 14a) is a surface which truncates both the Kibuye and Idjwi sedimentary sequences; the Iwawa-a sediments onlap this surface. There are other unconformities observed in the seismic record but the three described, H-1, H-2 and H-3, are widespread and display the most extensive truncation.

The Iwawa-a sub-sequence is the deepest of the three sequences which makeup the Iwawa Sequence. It is interpreted in the relatively high resolution SCS data to onlap the H-2 surface, and its upper sediments are subsequently truncated at the H-3 surface (Figs. 13b, 14b). A 10 m thick sedimentary sub-sequence, Iwawa-b, onlaps the H-3 surface (Figs. 13c, 14b). There is a high-amplitude reflective surface, H-4, that is observed throughout the basin in the CHIRP reflection data. This surface is part of the Iwawa-b Sequence and is deposited within 1 meter of the top of that sedimentary sequence. The H-4 surface onlaps the H-3 surface between ~380-395 m below modern lake level (MLL) (Figs. 13c, 14c). Sediments immediately above the H-4 horizon form the ~10 meter thick Iwawa-c Sequence, and these drape the sides of the basin up to at least 270 m below MLL (Fig. 14c). Shallow of the ~270 m isobath, basin slopes within the study area steeply inclined and sediments deposited here are unstable and disturbed.

The sedimentary sequences and surfaces are summarized here. There are three major sedimentary sequences resolved in the MCS data: Kibuye, Idjwi, and Iwawa; these are separated by two truncation surfaces: H-1 and H-2 (Fig. 16). The uppermost of these sections, the Iwawa Sequence, is divided into three sub-sequences including the Iwawa-a, Iwawa-b, and Iwawa-c Sequences as interpreted from the SCS and CHIRP seismic data (Fig. 16). Iwawa-a and Iwawa-b

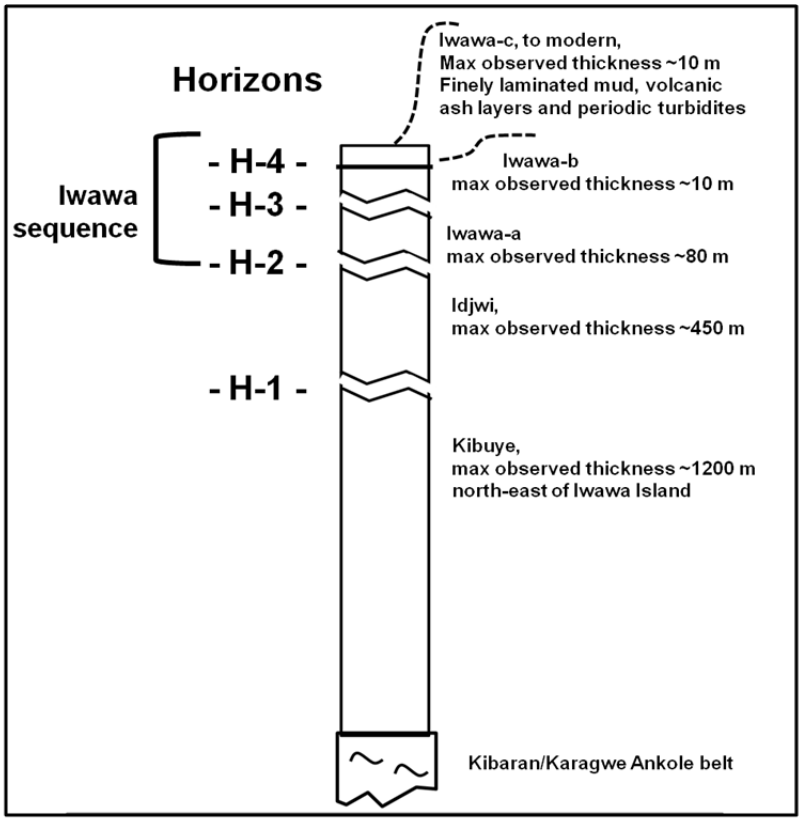

Figure 16. Sedimentary sequences identified in the eastern basin of Lake Kivu, interpreted from marine seismic reflection data. Iwawa sequence is divided into 3 sub-sequences. Horizons H-1, H-2 and H-3 surfaces exhibit truncated sediments. Horizon H-4 is a high-amplitude reflection which demarks a lake transgression at the end of the Iwawa-b lowstand. Note: not drawn to scale.

Sequences are separated by a truncation surface H-3, whereas Iwawa-b is distinguished from Iwawa-c Sequence section by a high-amplitude reflection surface, H-4, deposited near the top of the Iwawa-b sequence, a surface which onlaps the basin margin at ~390 m below MLL (Fig. 14c). The blanket of Iwawa-c sediments may be deposited up to the modern lake level, however, basin slopes shallow of ~270 m are too steep to support stable Iwawa-c Sequence sediments.

Om the southern end of the study area, the SCS and CHIRP profiles show deep incisions cut into the Iwawa-a, and Iwawa-b sequences (Fig. 14b, c). The maximum water depth shown in these profiles is ~405 m. The total Iwawa sediment sequence is less than 20 m thick across much of this profile except within the truncated channel shown near the left of the profiles; here, Iwawa sediments are up to ~50 m thick (Fig. 14b). Less than 25 m of Iwawa-a sub-sequence

remains below the H-3 truncation in the southern part of the study area (Fig. 14b) compared to the ~80 m observed in the north of the basin (Fig. 13b).

Parts of the study area that are less than ~450 m deep show a dendritic pattern of incisions into the underlying sediments (Fig. 15a). Some of these, south of Bugarura Island converge in a small basin offshore of the village of Kibuye, which has a depth of ~310 m below MLL (Figs. 14c, 15a). There is a notch in the western footwall of this small basin that connects these channels to the deeper, eastern basin of the lake (Figs. 1, 15a).

Six sediment cores with lengths between 6.5 and 8.5 m were acquired from water depths between ~325 and ~385 m (Fig. 17, Table 3). Most of the sediment recovered in each of these cores contains laminated mud interleaved with layers of volcanic ash and diatomaceous ooze (Fig. 18); these strata are easily correlated between cores across the basin. Volcanic ash layers within the cores show strong magnetic susceptibility and correlate to high-amplitude reflections in the CHIRP reflection seismic data (Fig. 18). As many as 22 distinct volcanic ash layers, ranging in thickness from >1 cm to <1 mm were observed along the ~9m length of a core. These ash layers indicate that at least as many volcanic eruptions occurred locally during the deposition time of these sediments. Seven of these ash layers ccorrelate to exceptionally high-amplitude reflection surfaces in the CHIRP data are identified in core 19 (Fig. 18). Each of the six cores terminates on a hard substrate of carbonate ooids or siliciclastic sand. In each core, a layer of homogeneous mud is deposited directly above the hard substrate. At the top surface of the homogeneous mud, there is a transition to fine laminations of mud, diatom-rich mud, and volcanic ash. These laminations are from ~1cm to <1mm thick, and constitute most of the length of each core (Fig. 18). The top of each core contains ~1 m of water-saturated, disturbed mud (Fig. 18).

Table 3. Characteristics of five sediment cores which recovered ooid samples, see map (Fig. 17) for core locations. Three left columns are profile characteristics interpreted from CHIRP seismic data at each core location (Fig. 27) The difference between the downcore depth and the CHIRP profile depth to the ooid layer in cores 5A and 17C is likely due to lost upper sediments during core recovery due to the core barrel over penetrating the sediments.

Core	Acquisition Date	Water Depth (m)	Downcore to ooids (m)	Depth to ooids	To Ooids, WD+ downcore	Lat.	Lon.	CHIRP TWTT to ooids (ms)	CHIRP Depth to Ooids (m)	CHIRP sediment depth to Iwawa-b (m)
KIVU13-12C	3/27/2013	385	7.7	392.7	392.7	-1.9376	29.2086	522	392	7.7
KIVU13-5A	3/15/2013	361	6.4	367.4	367.4	-2.0510	29.2278	499	374	8.2
KIVU12-14A	1/16/2012	356	8	364	364	-1.9779	29.2248	493	370	7.7
KIVU12-17C	1/18/2012	365	7.5	372.5	372.5	-2.0786	29.1794	504	378	9.0
KIVU12-19A	1/18/2012	352	8.5	360.5	360.5	-2.0851	29.2156	490	368	8.5

Carbonate ooids were recovered from near the bottom of five of the deep water sediment cores (Figs. 18, 19). These ooids were recovered from sedimentary strata that range from ~390-360 m below MLL, and from ~6.5-8.5 m downcore (Table 3). The locations where ooids were recovered correlate to a series of truncated terraces cut into the H-3 surface that is observed in the CHIRP data (Figs. 20b, 21a). The downcore distance to the ooid surface for cores KIVU12-14A (14A) and KIVU12-17C (17C) is less than the sediment thickness observed above the ooids as indicated by CHIRP data (Table 3). This discrepancy is due to sediment over-penetration of the core barrel and loss of the uppermost sediments during coring. The homogeneous mud layer above the ooid strata is <10 cm thick at core locations KIVU12-14A, KIVU12-19A (19A) and KIVU13-5A (5A), but in core KIVU13-12C (12C) the same massive mud layer is ~22 cm thick, and in 17C it is ~80 cm thick (Fig. 19). Core 5A penetrated through the relatively hard ooid layer to recover unconsolidated fine sand and gravel from below the H-3 truncation surface, this sand is interpreted to be from the uppermost Iwawa-b sequence (Figs. 20, 22).

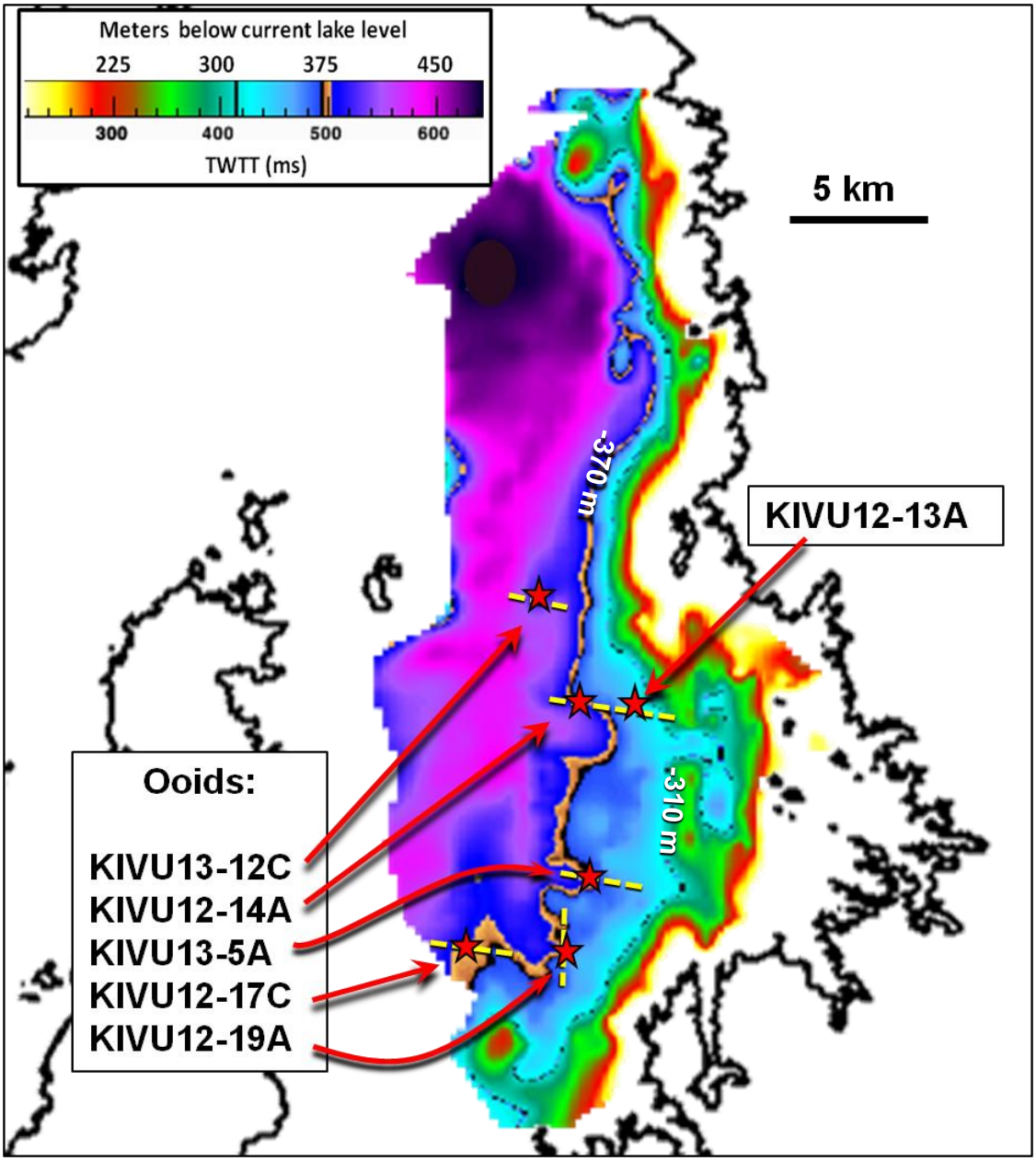

Figure 17. Structure contour map of the H-3 truncation surface showing locations of sediment cores . Stars are core locations, dashed yellow lines are adjacent CHIRP survey lines shown in figures 22 and 25. Orange and black contour is the 390-370 meter isobath and the approximate height of the Iwawa-b lake lowstand. Note: the 310 m isobath interpreted to be the approximate lake level during the earlier Iwawa-a, Idjwi, and Kibuye lake periods, is also shown.

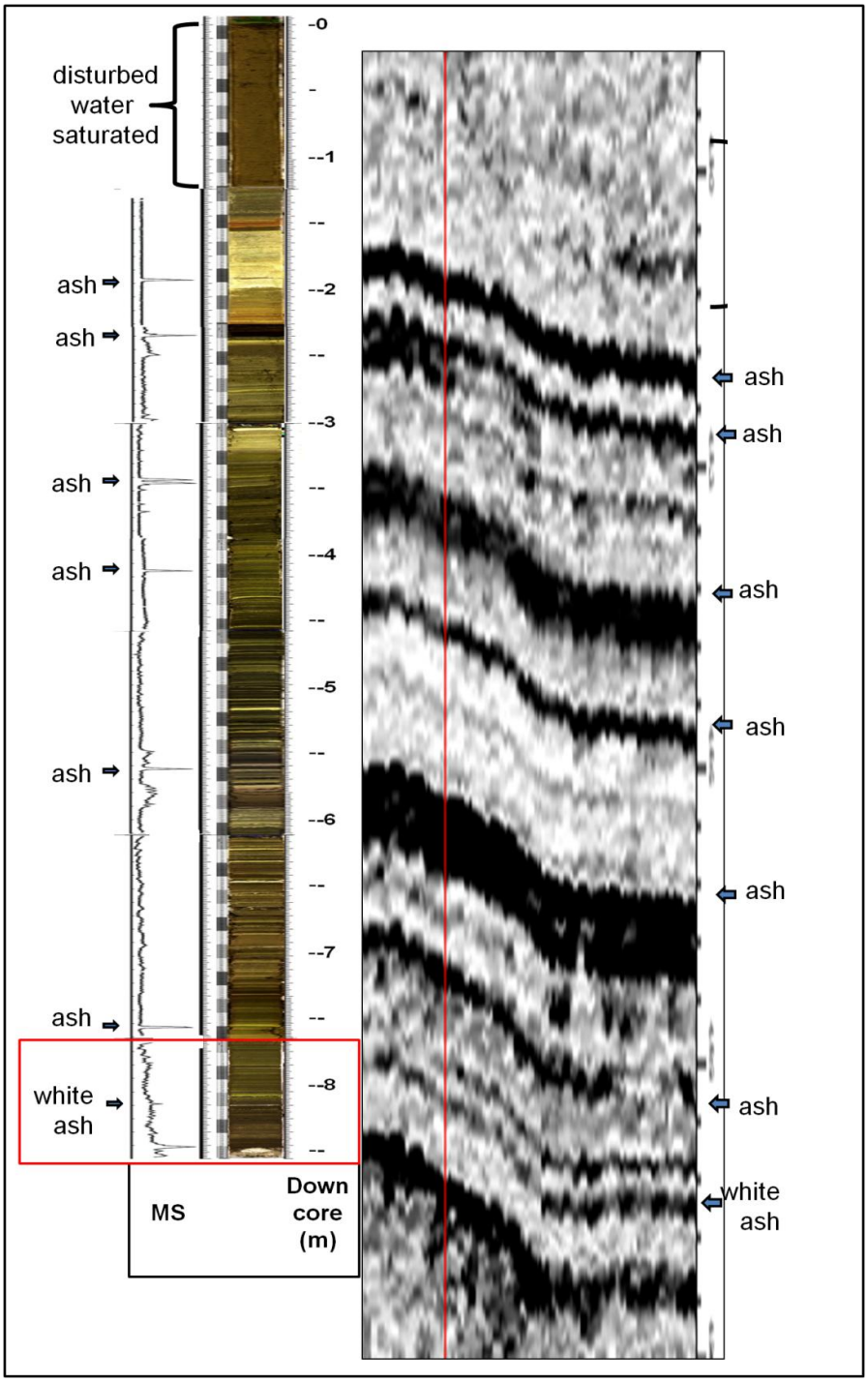

Figure 18. Image of core KIVU12-19A correlated to CHIRP profile KIVU12-C-06 adjacent to core site. MS = magnetic susceptibility. Large MS spikes correlate to thick volcanic ash deposits and high-amplitude reflections in CHIRP data Red rectangle at the base of the core image is the section shown in figure 19. Note: horizontal exaggeration on core image ~6x. See figure 17 for core location.

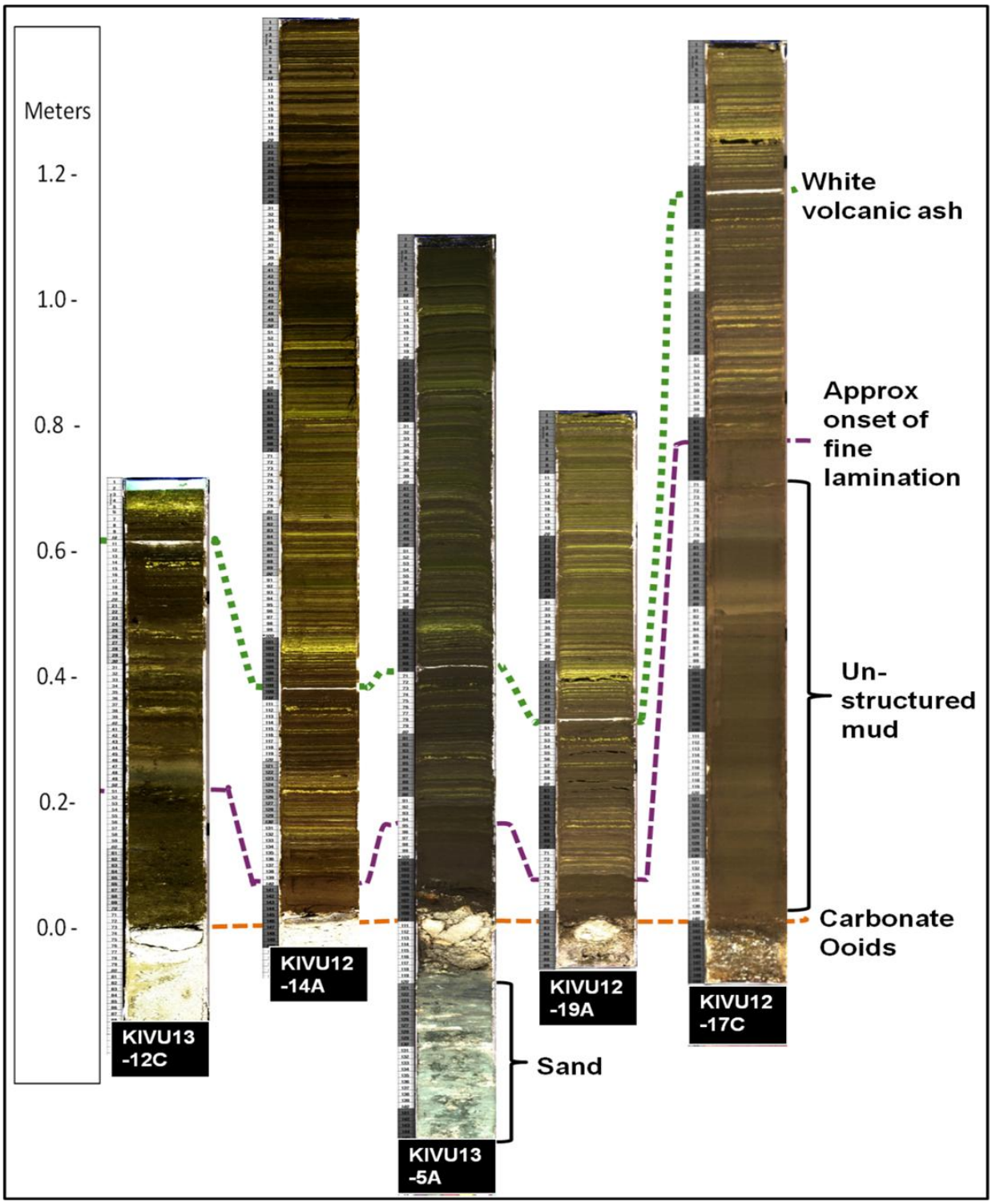

Figure 19. Lower sections of cores KIVU13-12C, KIVU12-14A, KIVU13-5A, KIVU12-19A, and KIVU12-17C; see table 3 for core background data and figure 17 for location map. The transition from unstructured, homogeneous clay to fine lamination occurs within <20 cm of the ooids in each core except for KIVU12-17C where the homogeneous clay deposit is ~80 cm thick. The white volcanic ash layer ~40 cm above the onset of lamination, is easially correlated across these cores, core 13A (Fig. 22), and it is observed in the CHIRP data (Figs. 18, 27). Note: ~2x horizontal exaggeration on core images.

Organic macrophytes recovered from the cores were radiometrically dated and stratigraphically correlated between cores in order to interpolate the age of the Iwawa-c Sequence and time since the ooid deposition. Earlier work resulted in anomalously old ^{14}C radiometric ages on shells due to the input of old carbon from CO_2 injected into the lake from hydrothermal springs (Tietze et al., 1980), as a result, only radiometric ages from terrigenous organic matter recovered from the sediment cores are presented in this study. Fifteen terrestrial samples from various cores were dated and cross correlated to core 19A (Table 2).

Core KIVU12-13A (13A) penetrated the entire Iwawa-c sedimentary record and recovered sand and gravel from below the H-3 surface (Figs. 21, 22). This core is from a water depth of ~330 m which is bathymetrically ~40-60 meters higher than the cores that recovered ooids. Above the sand layer in core 13A, there is ~4 cm of homogenous mud below the transition to fine laminations (Fig. 22). Proceeding from the location of core 14A, eastward and upslope along line KIVU10-22, there is little observed change in the appearance of the Iwawa-c Sequence sediments, and no observed onlap onto the H-3 surface in the CHIRP data shallow of the highest occurrence of the H-4 surface (Fig. 21).

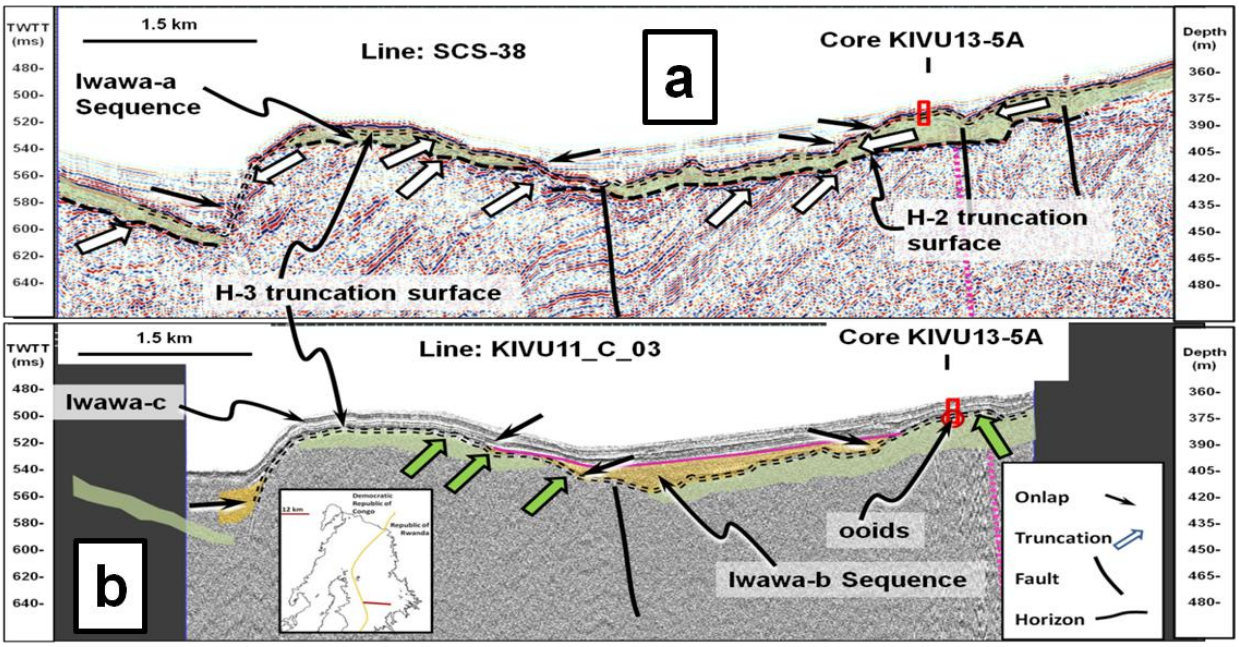

Figure 20. Coincident lines SCS-38 (a), and CHIRP line KIVU11_C_03 (b). The three Iwawa Sub-sequences are exhibited along with the location of core KIVU13-5A. Green shaded area in both profiles show the Iwawa-a Sequence; orange is Iwawa-b Sequence sediments. Truncation surface H-2 is the dashed line in the SCS profile. Truncation surface H-3 is the double dashed line in both profiles. Reflection surface H-4 (pink line) onlaps H-3 in the CHIRP profile. Green arrows show locations of terraces. Note: equal vertical scales in the profiles.

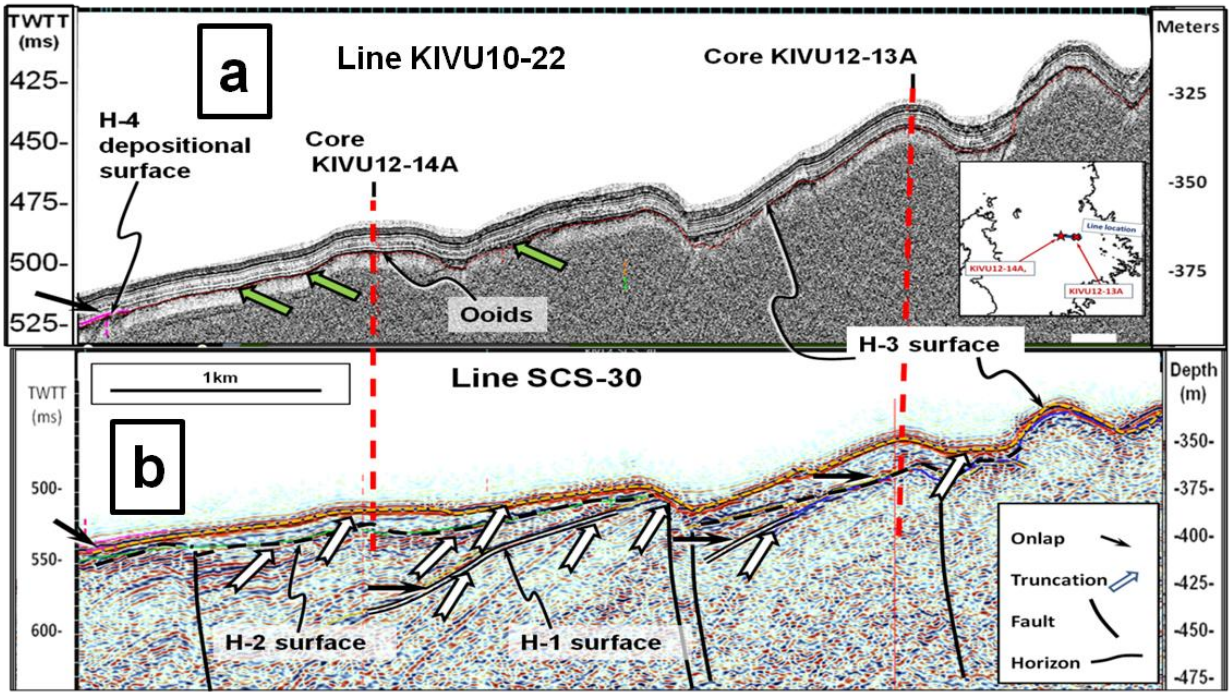

Figure 21. Coincident lines CHIRP KIVU10-22 (a), and SCS-30 (b). Vertical dashed lines show the locations of sediment cores KIVU12-14A and KIVU12-13A. The H-3 surface is represented by the dashed orange line in the SCS profile and is the acoustic basement of the CHIRP profile. Green truncation arrows in the CHIRP profile show locations of wave truncated benches. Note expanded scale on the CHIRP profile.

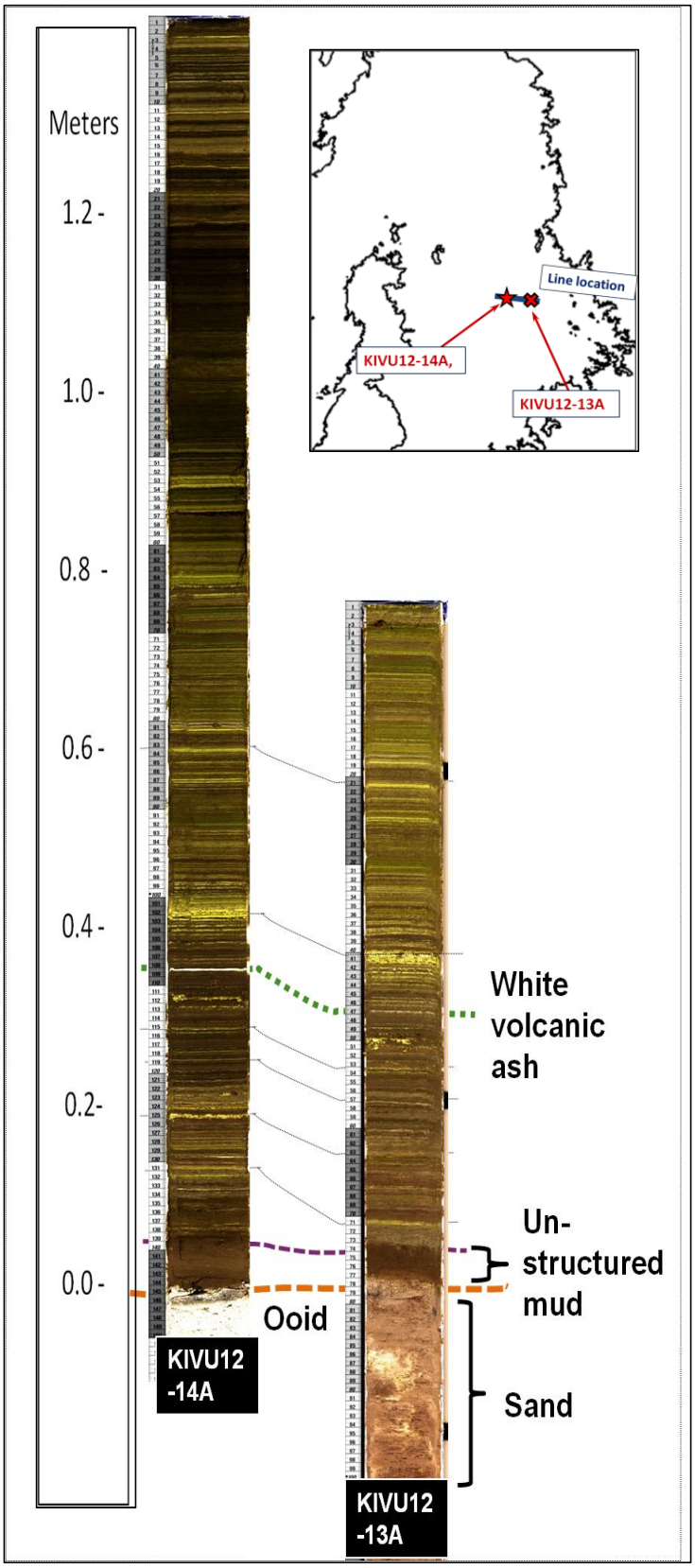

Figure 22. Images from core KIVU12-14A recovered from a water depth of ~362 m, and core KIVU12-13A from a depth of ~325 m; inset map shows locations of cores and seismic profile KIVU10-22, which these cores fall along. The base of KIVU12-14A contains ooids and the base of 13A contains sand. Note that the layer of homogenous mud deposited above the ooids and sand is approximately the same thickness in each core. Also note: laminated sediments beginning ~13 cm above the ooids in core 14A correlate to those beginning at ~7 cm above the sand in core 13A. This indicates that the deep conditions which allow preservation of fine lamina occurred at core site 14A before core site 13A.

Identifying the highest deposited sediments from each stratigraphic sequence reveals the minimum lake level during their deposition. Kibuye Sequence deposits are observed as shallow as ~320 m below MLL in line MCS-30 along the eastern side of the basin (Fig. 23a); these values do not take into consideration structural subsidence or uplift since deposition. Toward the north of the basin, there is a package of prograding reflections deposited on top of the H-1 surface (Fig. 23b). This south-dipping clinoform is ~150 m high, extends ~2 km horizontally, and contains topset deposits at ~550 m below MLL (Fig. 23b). Idjwi Sequence sediments onlap this delta and are observed onlapping the H-1 surface up to a maximum height of ~320 m below MLL. Above the Idjwi Sequence, the Iwawa-a sediments onlap the H-2 surface and are observed as high as ~320 m below MLL in line SCS-103 (Fig. 24c). The Iwawa-b Sequence sediments reach a thickness of ~10 m, and onlap the H-3 surface up to a maximum height of ~380 m below MLL (Figs. 14c, 20b, 21a, 24d). This is ~60 m lower than deposits observed to be from the earlier sedimentary sequences. The blanket of Iwawa-c sequence sediments is ~10 m thick and is draped above the Iwawa-b Sequence and H-3 surface (Figs. 21a, 24d).

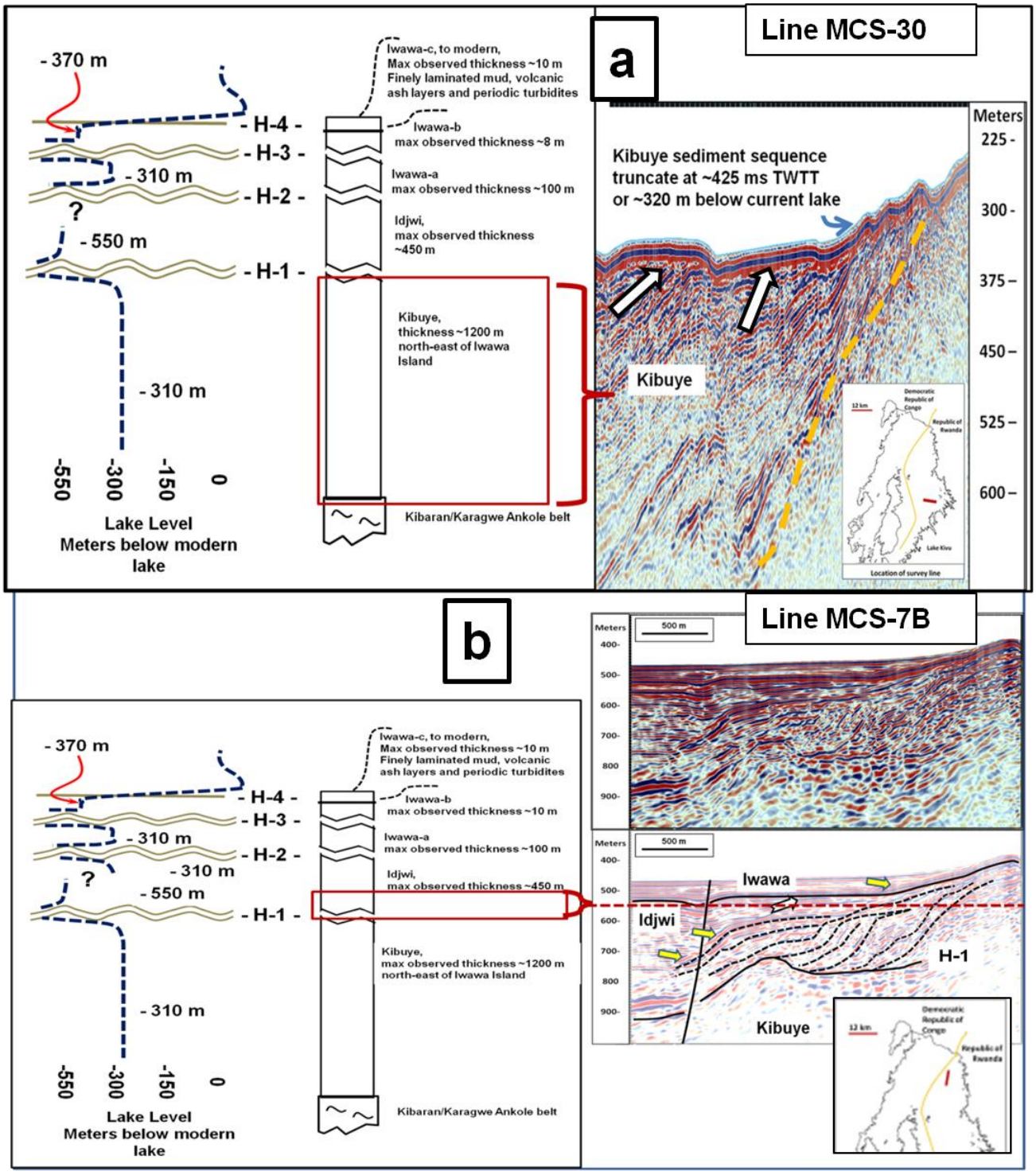

Figure 23. Lake surface level estimates for each sedimentary sequence based on the maximum height of observed sediments. Left column in each panel shows the approximate lake level, image to right of each panel shows the sediments in profile. Kibuye Sequence is observed truncated up to ~320 m below modern lake level (MLL) (a). Paleodelta deposited above surface H-1 during a lake lowstand of ~550 m below MLL (b). Newer Idjwi sediments onlap this delta (yellow arrows). Idjwi Sequence sediments are observed up to ~320 m below MLL.

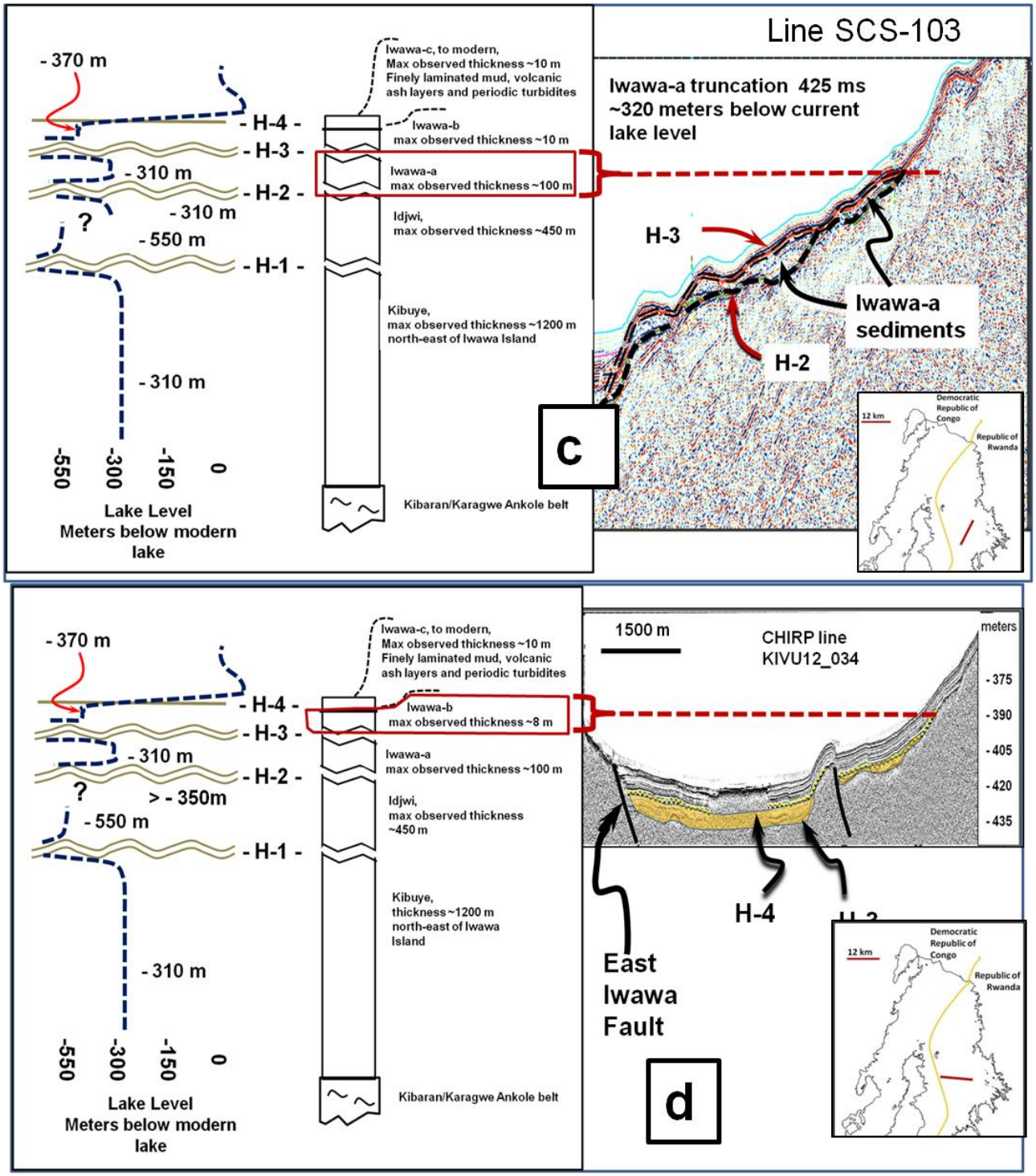

Figure 24. Lake level estimates continued from figure 23. Iwawa-a sediments observed at ~320 m below MLL, (c). Iwawa-b sediments (highlighted in orange) onlap the basin only up to ~390 m below MLL (e), this indicates that the Iwawa-b lake stand was ~60-80 m lower than the earlier lake periods underfilling the basin. Iwawa-c, the youngest sediment sequence is draped above Iwawa-b. Note the steeply inclined basin slopes shallow of ~370 m.

Discussion: Basin Structure

The structure of the eastern basin of Lake Kivu is dominated primarily by two north-south striking faults along the basin's western margin and east of Iwawa and Idjwi Islands (Fig. 6). Most extension observed within the study area is accommodated along the East Iwawa Basin Fault (EIF) east of Iwawa Island and located on the west side of the basin (Figs. 6, 7a, b, 8). The bathymetric high on the west side of profiles MCS-22 and MCS-18 is the northern extension of the Idjwi Island crystalline horst (Figs. 6, 7b). The throw of this fault exceeds ~2 km, which is interpreted as the sum of denudation of the upper footwall, water depth, and sediment deposited above the hanging wall (fig. 6). Observed at line MCS-20, the EIF is a listric fault that dips eastward at ~50º near the lake bed, then the dip angle appears to shallow to ~ 40º from 1000-1500 m below the lake bottom (Fig. 6); some of this change in observed dip could be due to error in the sound velocity estimate for the deeper sediments. Synthetic, intrabasinal faults also appear to decrease their dip angles with increasing depth (Figs. 6, 7). The sedimentary section in the west dipping hanging wall tends to dip more steeply in the northern part of the basin which is narrower. South of Iwawa Island the basin is wider and the average hanging wall dip decreases to ~6º exhibited on line MCS-36 (Fig. 7c).

The dip angles of the sedimentary strata next to the EIF decrease gradually up section (Fig. 6), indicating growth fault activity since the onset of sedimentation. Displacement across the most recent, uppermost sediments, and a 60 m escarpment at the lake bottom formed by the EIF show that the fault has recently been active (Fig. 7b). The Central Basin fault exhibits displacement of >100 m in the older strata, but there is less displacement of the upper stratal surfaces, and the escarpment at the lake bottom is only 5 m high.

Most basin subsidence south of Iwawa Island is accommodated on a normal fault to the west of the study area interpreted from bathymetry (Fig. 8) (Zal, 2013). The EIF is present on lines MCS-22, MCS-14, and MCS-18 (Figs. 7, 8a, 8b), but it is not observed on line MCS- 36 (Fig. 7c). The southern terminus of this fault segment is southeast of Iwawa Island and north of line MCS-36. The segment is at least 20 km long (Fig. 8), but may extend farther north, outside of the study area. Basin extension south of Iwawa Island is accommodated by a fault on the east side of Idjwi Island in the DRC. A northeast striking, oblique transfer fault is interpreted to connect the fault east of Idjwi Island to the EIF, and slip along this transfer fault accommodates the strain between these two faults (Fig. 8). The assumed average basement dip south of Iwawa Island is ~6º. If this dip continues on the western side of the international border, then by extrapolation, the basement is interpreted to reach a depth of ~2200-2400 m below MLL in the DRC near Idjwi Island (Fig. 8).

Total extension across the entire Kivu Rift Eastern basin includes the sum of the extension across the eastern and western basins, as well as onshore parts of the basin. The MCS data constrain most extension accommodated across the eastern lake basin, but in the absence of similar data in the northern basin, fault heaves must be estimated from topography and bathymetry. Observed eastern basin extension, interpreted as horizontal displacement of the basement, is up to ~2.1 km along line MCS-14, and mostly is accommodated by heave along the EIF (Fig. 7a).

The border fault system on the northwestern side of the lake is the primary control of the shape of the Kivu Rift (Ebinger, 1989a). Displacement on this fault system is estimated as the sum of the sediment thickness, water depth above the fault's hanging wall, and the ~1 km escarpment above the lake, which is eastern slope of this segment of the Mitumba Mountain

Range. No reflection seismic data is available near the lake's western shore to ascertain the maximum sediment thickness near the border faults. Interpolating from the MCS data acquired in the eastern basin, sediments near the western border fault could be considerably thicker than those in the eastern basin. Accordingly, subsidence in the western border fault could be much greater than the amount accommodated in the eastern basin. Assuming that extension accommodated west of Idjwi Island exceeds the ~2.1 km observed in the eastern basin by MCS data, the upper crustal extension across the Kivu Rift is > 5 km.

The three northernmost faults described in the MCS data strike to the northeast (Fig. 8). These fault segments probably extend outside of the study area and are sub-parallel to the oblique transfer fault which is south of Iwawa Island which is interpreted to transfer strain from the EIF to the margin fault east of Idjwi Island (Fig. 8). These three northern faults exhibit >100 m of displacement in deeper sediments but show little recent activity; they may be formed from an earlier episode of northwest-southeast directed basin extension. Accommodation of newer, east-west extension, as oblique strike-slip along older, northeast striking faults and fractures could account for the irregular, zig-zag shape of Kivu's basins and islands.

Discussion: Stratigraphy

The sediments of Lake Kivu reveal a dynamic lake level history, and past lake level information recorded within lake sediments are a sensitive proxy for a region's paleoclimate and tectonic history (e.g., Carroll and Bohacs, 1999; Johnson, 1996; Johnson et al., 1996; Scholz, 2002). Tropical Rift Valley lakes show extreme variations in water volume in response to climate changes (e.g., Scholz and Rosendhal, 1988). Stratal relationships, paleoshorelines, and

the position of the highest draping sediments in the basin help determine past lake levels. Comparing the timing of changes in Kivu water level to those in other regional lakes can also help to separate tectonic and climate signals.

The Kibuye Sedimentary Sequence (Fig. 10) comprises most of the sedimentary section in the East Kivu Graben. Accordingly it represents most of the basin's depositional history. The thickest Kibuye sediments are observed northeast of Iwawa Island, bordering the EIF at the point of the fault's maximum displacement (Fig. 10). These sediments are estimated to be thicker on the DRC side of the basin south-west of Iwawa Island. The highest Kibuye sediments are observed deposited up to 320 m below MLL (Fig. 23a). This indicates that the lake surface was above this depth, ~310 m below MLL, during some, or all of the Kibuye deposition. A component of the Kibuye Sequence material was lost to erosion, and the overall basin uplift or subsidence since deposition cannot be measured. Accordingly it is not possible to assess the uncertainty of this lake level estimate, or to determine how much variation in lake level occurred during the Kibuye period. This value of ~310 m below MLL is interpreted to be the lake level during the Kibuye lake stage based on the available data.

The Kibuye Sequence is truncated along its upper surface by the erosional surface H-1 (Figs. 6, 7). The H-1 unconformity is interpreted across the entire study area, including the deepest, northern part of the basin. This indicates that the entire study area in the eastern basin of the lake was desiccated after Kibuye Sequence deposition.

An underfilled lake basin may rapidly alternate between desiccation and flooding (Carroll and Bohacs, 1999), and this describes the lake's transgression following the H-1 desiccation event. The paleodelta in the north of the survey area (Fig. 23b) onlaps the H-1 surface and has a

topset reflection at ~550 m below MLL. The depth of the topset of this clinoform will be near the water surface during deposition, indicating that the lake stood at, or above 550 m below MLL depth for long enough to build this structure after the H-1 desiccation. This depth estimate, however, does not account for subsequent subsidence of the structure. Upper Idjwi Sequence sediments onlap the foreset surface of this structure (Fig. 23b), indicating that the lake surface regressed then transgressed at least once after the delta's formation. This clinoform deposit was probably connected to either the ancestral Sebeya Stream, or other larger watershed systems currently buried under the Virunga Volcanics.

Idjwi Sequence sediments onlap the paleodelta (Fig. 23b) and are observed to onlap the H-1 surface up to 320 m below MLL. It appears that after the event which initiated the H-1 desiccation, the lake eventually recovered to the level of the earlier Kibuye Sequence time. The Idjwi Sequence is thickest in the northwestern corner of the study area (Fig. 11). South of line SCS-22, the wedge of Idjwi Sequence sediments is half as thick as it is north of the line (Fig. 11). Currently, the water depth in the southern part of the basin is shallower than the northern area (Fig. 1), and unless there has been greater subsidence near the north end of the lake since their deposition, the southern Idjwi Sequence sediments have been subaerially exposed for longer durations than those to the north. A consequence of this extra exposure is that Idjwi and Iwawa sediments in the south are thinner and more deeply incised than sediments in the north of the study area (Fig. 14b, 21a).

The Idjwi Sequence is truncated along its upper surface by the H-2 surface which is interpreted to be an exposure surface (Figs. 6, 7, 13, 14). The high angle unconformity at the H-2 surface (Fig. 6) indicates that a large quantity of material was lost to erosion here. H-2 desiccation appears to be the most prolonged arid period recorded in these seismic profiles.

Iwawa-a sediments onlap the H-2 surface (Figs. 13b, 21b), indicating that lake level rose gradually after the H-2 desiccation event. Traces of the Iwawa-a sequence are observed as far up the basin side as ~320 m below MLL (Fig. 24c). This indicates that the lake again returned to the level of earlier Idjwi and Kibuye Lake stands. Iwawa-a Sub-sequence sediments are ~80 m thick in the north of the basin, where they are minimally truncated by the subsequent H-3 desiccation event (Fig. 13b). This part of the basin may have remained subaqueous during most of the H-3 desiccation period. Iwawa-a Sequence sediments in the southern part of the basin are generally less than ~20 m thick, and are deeply incised by erosional channels (Fig. 14b, 20a). These incisions are subaqueous channel extensions of onshore streams eroded during lake low stands or desiccation events (Fig. 15a). These channels currently serve as conduits for subaqueous density flow currents (Fig. 15).

Following the H-3 desiccation event, the lake did not rise to the former minimum lake level of ~310 m below MLL; Iwawa-b Sequence sediments onlap the H-3 surface only up to ~380m below MLL (Fig. 24d). None of the cores intersect the H-4 surface, however, it is interpreted as a layer of water-lain volcanic ash based upon its similarity to other reflections which are correlated to ash samples in sediment cores (Fig. 18). It is deposited near the top of Iwawa-b Sequence sediments and onlaps H-3 between ~395-380 m below MLL (Figs. 20b, 24d). Terraces observed in the H-3 surface between ~385-370 m below MLL are erosional benches incised into older sediments during the Iwawa-b lake lowstand (Figs. 14c, 20b, 21a). These terraces are interpreted as erosional features created by surface wave activity near a shoreline, and accordingly reveal the level of the lake surface during the Iwawa-b lake stage. These show that the lake varied between ~385-370 m below MLL during that period (Fig. 25). The Iwawa-b period lake is between ~80 to 60 m lower than the earlier lake stands, but was still a ~100 m deep

lake. The Iwawa-b stage is considered to be 370 m below MLL, which corresponds to the highest observed eroded terrace.

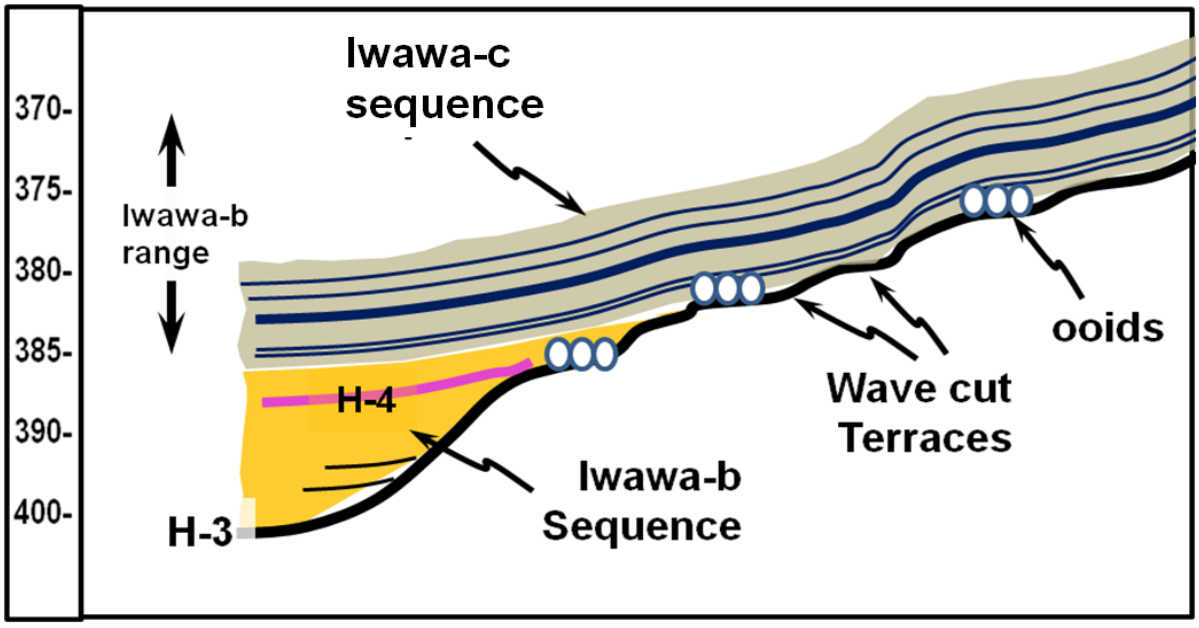

Figure 25. Schematic diagram showing erosional and depositional features from the Iwawa-b (orange), and Iwawa-c (grey) Sequence lake periods. H-3 is the truncated surface that these sediments are deposited above; H-4 is interpreted to be a reflective volcanic ash layer deposited near the top of the Iwawa-b Sequence sediments. Three circles represent shallow water carbonate ooid deposits. The early Iwawa-b lake surface was ~385 m below current lake level, at this time the lowest (left most) bench was eroded into older sediments. During a gradual, ~15 m lake level rise, surface wave activity formed progressively higher terraces on the H-3 surface. These terraces accommodated shallow water ooid production which progressed shoreward as the lake level rose. Some earlier ooids would be buried by newer Iwawa-b Sequence mud as the water deepened at their location. Iwawa-c Sequence sediments are deposited above after a rapid, >400 m lake level transgression.

Discussion: Sediment Core-Seismic Correlations

Most of the sedimentary section recovered from the six described Kullenberg sediment cores consists of laminated mud and biogenic material deposited during the Iwawa-c period of the lake (Fig. 18). Exceptions are the sandy sections from the bases of cores 5A and 13A, the basal ooids from five cores, and some of the homogenized mud deposited directly above the ooids in core 17C (Figs. 19, 22); these specific materials were deposited during earlier lake

sequences. The uppermost ~1-1.5 m section of each core, exhibited in core 19A (Fig. 18), is mud disturbed by degassing during the core's recovery. The density of this uppermost, high water content section is very low, making it nearly transparent in the seismic data (Fig. 18). Excellent preservation of the fine lamina throughout most of the core indicates deep water, anoxic conditions at this location preventing disturbance by benthic organisms or surface wave activity. The sand sections recovered from the bottoms of cores 5A and 13A (Figs. 19, 22) are from below the H-3 exposure surface and belong to the Iwawa-a sedimentary sequence (Figs. 20. 21).

Carbonate lacustrine ooid formation is restricted to shallow littoral regions (Wilkinson et al., 1980); accordingly, ooids recovered by five sediment cores from the benches formed on surface H-3 indicate that the lake surface was at approximately this depth at their time of their formation. Ooids in Cores 14A, 19A, and 5A are recovered from near the east shore of the paleolake (Fig. 17). These three eastern samples come from depths between ~374-368 m below MLL, a range of ~6 m (Table 3, Fig. 26). Core 17C, from the south shore of the paleolake, and west of the three east shore cores (Fig. 17), recovered ooids from ~380 m below MLL, this is 6-12 m lower than the eastern shore samples. The high-amplitude reflection H-4, presumed to be a layer of volcanic ash, was deposited after a volcanic eruption and represents an instantaneous depositional event near the end of the Iwawa-b lake period. Ooids from core 17C were ~1-2 m higher than the nearby H-4 onlapping surface (Fig. 26d), whereas the eastern ooid samples were recovered from ~5-14 m above the same reflective surface (Figs. 26a,b,c). This relative vertical proximity to the H-4 surface indicates that ooids from 17C were formed close to H-4 ash deposition time, and earlier than the eastern ooids. There is also ~80 cm of homogenized mud

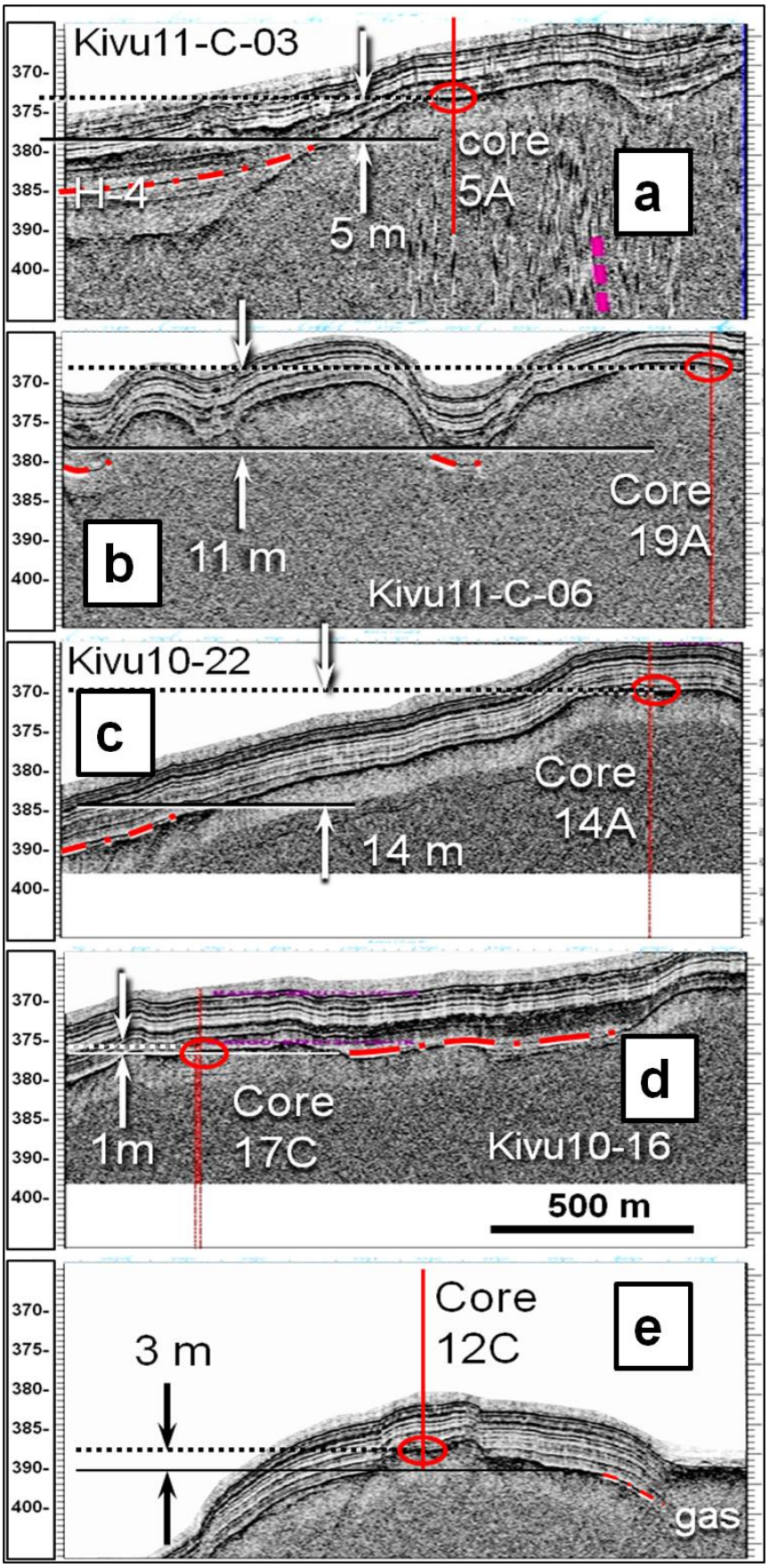

Figure 26. CHIRP profiles near the five core sites which recovered ooids showing relative vertical distance between the ooids and onlap of surface H-4 (see map Fig.17 for core locations). Vertical red lines are the core locations, red ovals indicate recovered ooid deposits, and the dashed red line is the H-4 high-amplitude reflection surface (volcanic ash) which onlaps below the ooids near each core. Horizontal dashed line is the level of the ooid deposit; solid line is the level of the nearest onlapping H-4 sediments. Note that the ooids from cores 17C and 12C are deposited within 1-3 m vertically to the H-4 surface, whereas the three eastern shore cores show ooids which are >5 m above the onlapping H-4 surface. Vertical scale is in meters below the current lake surface.

deposited above the ooids in core 17C, whereas the three samples from eastern shore benches have less than ~10 cm of similar mud above the ooids (Fig. 19). Ooids from core17C are interpreted as having formed on a shallow, wave cut terrace which became unsuitable for ooid production after a lake rise of ~10 m during the Iwawa-b period (Fig. 25). The belt of ooid production migrated shoreward as the Iwawa-b lake level rose; this is indicated by the higher wave cut benches with newer ooid deposits. Most of the ~80 cm of massive, unstructured mud above the ooids in core 17 C was deposited during the Iwawa-b lake stand when the lake rose slightly to produce the higher benches. The homogenous mud above the ooids in core 17C shows no clear boundary between the sections deposited during the Iwawa-b and Iwawa-c periods. Until the lake rose to a level where benthic water at this location became anoxic, sediments were be mixed by benthic invertebrates.

Ooids from core 12C were recovered from ~392 m below MLL which is deeper than core 17C is (Table 3, Fig. 26d,e). These ooids were recovered from a paleoshoal, located between Iwawa and Bugaura Islands (Fig. 17). As with core 17C, the ooids from core 12C were recovered from a terrace in close vertical proximity to the nearest H-4 onlapping surface (Fig. 26e) indicating that this sample was deposited at about the same time as 17C, and earlier than those of the three eastern shore samples. The high-amplitude reflection, H-4, onlaps >5 m lower near core 12C than it does near the other core locations (Fig. 26). If this deposit onlapped up to a specific depth below the lake level, then lower observed onlap of this surface indicates that there has been ~5 m greater subsidence at core site 12C than near the other core sites since the time of deposition.

The Iwawa-c Sequence, which includes the modern lake deposits and high stands above the modern lake stand, drapes above the Iwawa-b sequence and the H-3 truncation surface (Figs.

20b, 21a). The earliest Iwawa-c Sequence sediments show that the transgression after the Iwawa-b lowstand occurred quickly. The white volcanic ash layer, which is <1m above the H-3 surface in all of the described cores (Figs. 18, 19, 22, 27), is identified and correlated to a reflective surface in the CHIRP data (Fig. 18). The continuity of this layer shows that the lowest meter of the Iwawa-c sediments is draped above the upper Iwawa-b, H-3 surface, and is observed as shallow as 320 m below MLL (Fig. 28). This white ash layer may have been initially deposited higher up the basin sides, however, slopes within the study area above the ~ 320 m isobath are too steep to support stable Iwawa-c sediments. The range of this lowest meter of Iwawa-c sediments shows that there was little onlapping above the Iwawa-b lake lowstand. Also, no shallow wave cut benches are observed eroded into the H-3 surface above those formed during the Iwawa-b lake stage. There is additional evidence of a rapid lake level transgression exhibited in sediment cores 14A, 19A, and 5A. These show changes over a short vertical distance, from the shallow, high-energy conditions necessary to produce ooids, to the deep, anoxic conditions necessary to preserve fine lamina. The unstructured layer of mud separating these two facies is less than ~10 cm in these cores (Fig.19). Core 13A was acquired from a depth ~40 m shallower than 14A (Table 3, Fig. 28), but shows a sequence of fine lamina starting ~7 cm above the sand; these fine lamina correlate precisely to those deposits starting ~15 cm above the ooids in the deeper water core (Figs. 22, 28c,d). The onset of deep water, anoxic conditions in core 13A occurred earlier, depositing ~5-7 cm of laminated sediment before matching deep water conditions reached the shallower core. After this time, the cores share a common depositional sequence. Iwawa-c sediments are disturbed shallow of the ~270 m isobath therefore it cannot be ascertained if this transgressive lake level pulse reached the lake's southern spill point from these data. Other Kivu sub-basins may show better sediment preservation above the 270 m isobath.

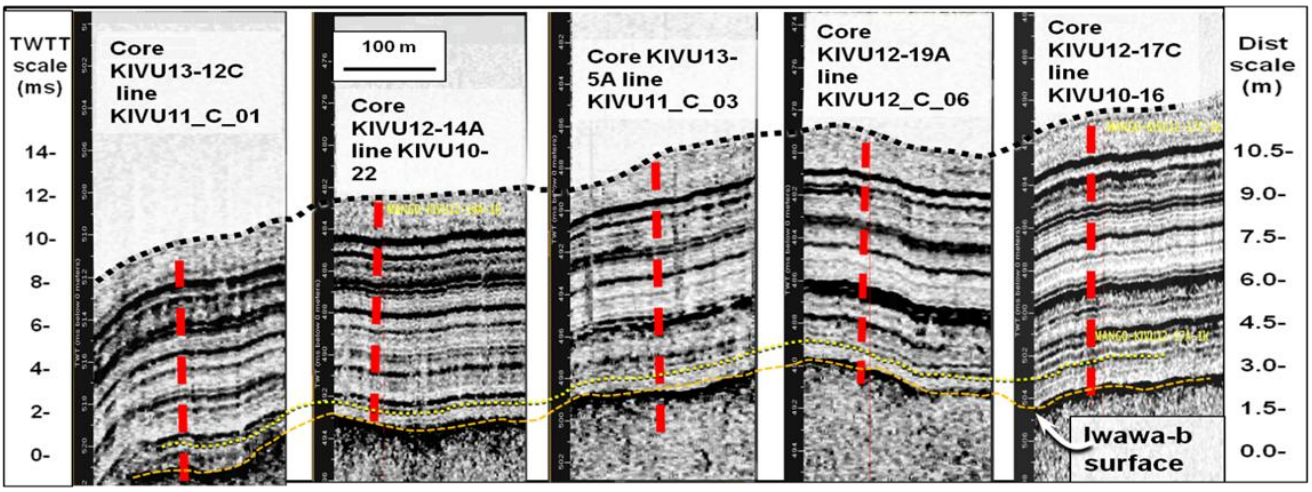

Figure 27. CHIRP profile sections at each of five core locations where ooids were recovered, see figure 17 for location map, and table three for core characteristics. Orange dashed line is the H-3 truncation surface, which is the acoustic basement for this seismic system; ooids are deposited on this surface. The yellow dashed line above is a reflection which correlates to the white volcanic ash layer (Fig. 19). Black dotted line is the approximate sediment-water interface; vertical dashed red lines are approximate core locations. Note: these profiles are at the same scale but have been moved vertically to show stratigraphic correlation.

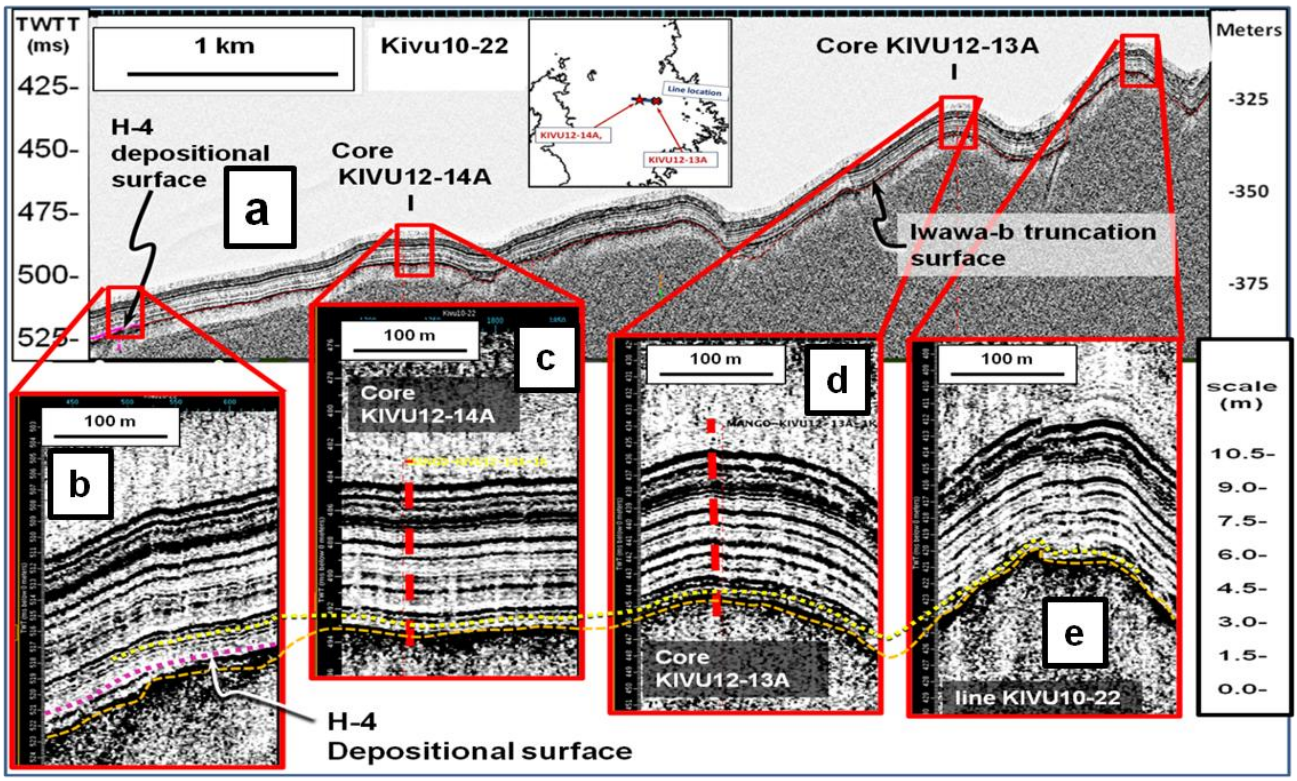

Figure 28. CHIRP profile KIVU10-22 (a), see inset map for location. The orange dashed line (panels b-e) represents the H-3 erosional surface, the yellow dotted line above it correlates to the white volcanic ash layer (Fig. 22). Core KIVU12-14A recovered ooids from the H-3 surface at ~370 m below MLL; core KIVU12-13A penetrated the H-3 surface at ~334 m below MLL, and recovered sand from underneath the surface. The high-amplitude reflective surface H-4 (pink dotted line in panel b) onlaps the H-3 surface at ~388 m below MLL. Profiles b-e are shown at equal scale but moved vertically to show stratigraphic correlation.

The following is a summary of Lake Kivu's level history: 1. Throughout most of Lake Kivu's history, as recorded by the Kibuye through Iwawa-a Sequences, the lake level was ~310 m above MLL between desiccation events (Figs. 23a,b, 24c). This consistent lake level is interpreted to correlate to the level of the basin spill point. This is interpreted as the level of a northern outlet reported in earlier work (e.g., Brooks, 1950; Degens et al., 1973; Haberyan and Hecky, 1987). 2. Sediments observed onlapping each exposure surface show that the lake level recovered from these dry climatic periods gradually, perhaps cycling between flooding and desiccation during each transgression. 3. The event represented by the H-2 truncation surface exhibits the most extensive angular unconformity and represents the most persistent arid period in the sedimentary record. 4. After the third desiccation event, H-3, the lake recovered to ~390 m below the current lake level, or ~80 m lower than the earlier lake stands (Fig. 24d). During this lowstand, interpreted as an arid climate period, the lake basin was underfilled and the lake's surface varied by more than 20 m, reaching ~370 m below MLL. 5. There was a rapid transgression at the end of this lake lowstand culminating in the deeper Iwawa-c lake stage.

Discussion: Chronology of Rifting and Lake Level Changes

The age of the uppermost, Iwawa-c period of the lake may be interpolated from radiometrically dated core samples. However, only surficial sedimentary material has been acquired from lake periods earlier than Iwawa-c so other methods must be used to estimate their ages. The fifteen dated samples removed from, or stratigraphically correlated to core 19A display a linear relationship between sediment age and downcore depth (Fig. 29). From these data, the average sedimentation rate for this core, and the Iwawa-c period, is ~0.7 m/ka. The age of the

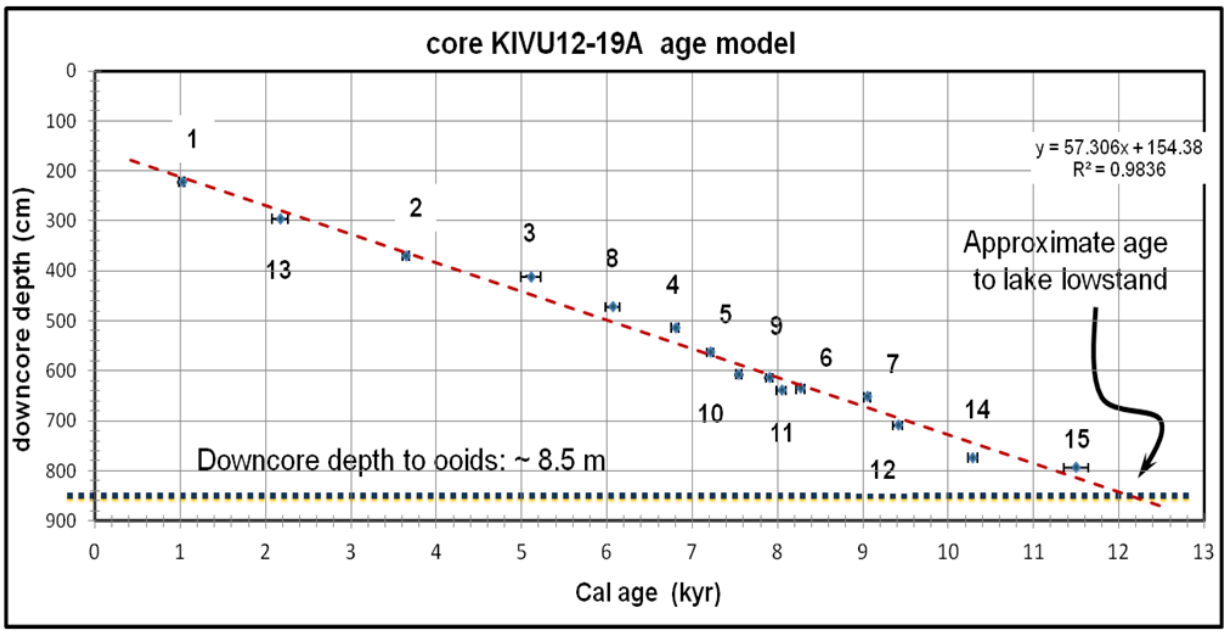

Figure 29. Radiocarbon ages of samples stratigraphically correlated to core KIVU12-19A. The downcore depth to the ooids deposited during the lake lowstand for this core is ~8.5 m (dashed line). See table 2 for sample descriptions.

ooid layer at this location, 8.5 m below the lake bed (Table 3), is therefore estimated at ~12 ka which is interpreted to be the end of the Iwawa-b lake stage and the onset of the transgression to the Iwawa-c lake level.

The thickness of the layer of unstructured mud deposited above the ooids during the transition between the Iwawa-b and Iwawa-c lake stages may be used to estimate the rate of the transgression from the Iwawa-b to the Iwawa-c lake stage. Cores 5A, 14A, and 19A, which do not have Iwawa-b Sequence sediments deposited above the ooids, exhibit ~5 to 10 cm of homogeneous mud separating the shallow water ooids from the deep water, laminated deposits (Fig.19). Assuming the homogenous mud accumulated at the average Iwawa-c sedimentation rate, this transition occurred over a period of ~70-140 years. Core 13A, which was acquired from ~40 m above the Iwawa-b lowstand contains ~4 cm of massive mud deposited during this lake level rise which indicates a ~60 year transgression at that location (Fig. 22). The additional ~5-7

cm of laminated material observed in core 14A, but is not present in core 13A (Fig. 22), implies that deep, anoxic conditions occurred at location 14A ~70-100 years before they did at core site 13A assuming that sedimentation rates are similar at each location. These data do not constrain the minimum depth required for fine lamina preservation. Additional data from shallower sediments are required to determine if this transgressive pulse rose above the current lake level. The current hydrologic budget for the lake basin suggests that this rapid lake transgression would have been possible if climate conditions were as wet as modern conditions. The volume of the modern lake is ~560 km^3, and the lake's outflow past the Rusizi 1 Hydropower Plant is ~3.6 km^3/yr (Muvundja et al., 2009). This annual outflow would fill the basin from empty, to its current level in ~160 years. At the onset of the transgression however, the lake was already ~100 m deep, but the lake would need to raise ~100 m above the MLL to reach the basin spill point before the Rusizi River incised a canyon at the south end of the lake. Conditions comparable to or wetter than the current climate would support a lake level transgression at the rate shown in this sedimentary record.

Earlier studies report the Holocene lake level transgression was caused from water impoundment by expansion of the Virunga Volcanics (e.g., Brooks, 1950; Hecky and Degens 1973; Haberyan and Hecky, 1987). A change in climate, however, is a more likely primary control of this event. A lake level rise of ~400 m within a time frame of ~100-200 years would imply a massive, short-term expansion of the Virunga Province. Such an event, although possible, seems unlikely and would leave a record of its occurrence throughout the region. Many other Rift Valley lakes also rose from long-term low stands at approximately 12 ka (Johnson et al., 1996; Scholz et al., 2003; Felton et al., 2007; Moernaut et al., 2010), implying that there was a regional control on lake levels at this time. Virunga expansion likely did not determine the time

of the transgression after the Iwawa-b lake stage, but had a role in controlling the height of the Iwawa-c lake surface. The persistent lake stand ~310 m below MLL during the Kibuye, Idjwi, and Iwawa-a lake stages indicates that there was a basin spill point, probably at the north end of the lake, at that height during those periods. During the Iwawa-b period, growth of the Virunga Complex raised the topographic threshold, blocking the northern lake outlet. Initiation of this magmatic growth might have been during, or prior to the Iwawa-b lake lowstand period. With the northern outlet blocked, the rising lake would reach a higher, southern basinal spill point out of the Bukavu Basin. Tighter age constraints on eruptive history of the Virunga Complex must be made to further test this hypothesis.

If the uncompacted thickness of a sedimentary sequence, and the average rate of sedimentation are known, then the age of the sequence may be calculated. Sedimentation rates of the sequences older than Iwawa-c cannot be measured directly with current available data, but rough estimates may be made. To make such estimates, current sedimentation rate, rates from other lakes, historic variation in basin shape, and climate must all be considered. Work from other lakes in the region shows that long-term sedimentation rates can range from as low as ~0.1-0.15 m/ka over isolated, deepwater horsts in Lake Tanganyika (Scholz et al., 2003; Felton et al., 2007), to ~2 m/ka in Lake Edward (Russell and Johnson, 2005), or as high as ~2.4-2.7 m/ka in Lake Turkana (Halfman and Johnson, 1988). Unlike Lakes Edward and Turkana, Lake Kivu does not have a large inflowing river delivering sediments into the basin, so Kivu sedimentation is likely to have a lower rate than in these two lakes; 2 m/ka is estimated as the maximum probable sedimentation rate for older Kivu lake stands. The Iwawa-b lake stage represents a lowstand, closed basin lake, resulting from an arid climate period. During this period, sediments deposited during earlier, higher lake stands were subaerially exposed, and slopes probably less

vegetated then the current lake shores. Erosion rates were likely very high, and accordingly sedimentation rates for the Iwawa-b lake stand are estimated at ~2 m/ka. Higher Iwawa-a, Idjwi and Kibuye lake stands were likely open basin lakes, implying wetter climate periods. Wetter conditions will support more vegetation on surrounding slopes, stabilizing them and lowering erosion rates. If the lake surface level during the Kibuye, Idjwi and Iwawa-a lake periods was ~310 m below the current lake level, then several current lake basins to the south and west of Idjwi Island would have been subaerial (Fig. 1). Accordingly, sedimentation rates during these times would be likely slightly higher than current sedimentation rates: ~1 m/ka. These values are used to estimate the ages of the various sedimentary sequences and times to the desiccation events (Fig. 30). These are first order estimates and do not consider sediment compaction, the sedimentary record lost during desiccation periods, tectonic changes to the basin or watersheds, or the probability that sedimentary packages are thicker outside of the study area in the DRC territorial waters.

From these estimates, the age to some of the exposure surfaces interpreted in the sediments of the eastern basin of Lake Kivu correlate to climate events recorded in other regional sedimentary records. The rapid lake level transgression at the end of the Iwawa-b lowstand, which occurred at ~12 ka correlates to the termination of the Younger Dryas or Greenland Stadial 1, a ~1 kyr dry period which ended at ~12 ka at Lake Challa, Tanzania (Moernaut et al., 2010), and ~12.3 ka off the northwest coast of Africa (deMenocal et al., 2000). The H-3 truncation is estimated to have ended ~17 ka (Fig. 30). This correlates to the age of the last glacial maximum (LGM), ~35-15 ka (Cohen, et al., 2007) an arid period in East Africa when many other regional lakes experienced low stands (e.g., Johnson et al., 1996; Scholz et al., 2003; Felton et al., 2007; Moernaut et al., 2010). During this time, Lake Victoria was likely

completely desiccated (Stager and Johnson, 2007). The H-2 truncation, which appears as the largest unconformity within this sedimentary record, is estimated to have ended at ~97 ka. This is within a the estimated period of a regional megadrought, reported to have begun ~135 ka and ended ~70 ka; during this time, surface levels of Lakes Malawi and Tanganyika reached levels >400 m below present (Cohen et al., 2007). This period is reported to be much more arid and persistent than the LGM (Cohen et al., 2007, Scholz et al., 2007). The H-1 desiccation period is estimated to have ended at ~550 ka; the northeast striking faults observed in the north of the study area exhibit ~50 m of displacement at this surface. This implies that either there was either northwest-southeast extension, or oblique-slip along these faults as recently as ~500 ka. The overall age of the deepest sediments observed in the basin is estimated to be ~2 Ma (Fig. 30).

A different method which may be used to estimate the minimum age of the eastern basin of the lake, and test the extrapolation technique described above, is to divide the rate of rifting by the total basin extension. Kinematic observations which measure crustal motion estimate the rate of rifting near Lake Kivu to be ~3.8 mm/yr (Stamps, et al., 2008). Approximately half of this strain, ~1.9 mm/yr, is presumed to be accommodated by faults east of Idjwi Island. The total maximum heave, observed as horizontal basement displacement in the MCS data, is ~2.1 km (Fig. 7a). The minimum age of the oldest sediments in the basin are therefore calculated to be at least ~1 Ma. This age is considerably lower than the extrapolated value, but it does not account for the probability that more than half of the Kivu Rift extension is accommodated west of Idjwi Island, that some sediment record is lost to erosion, and that some eastern basin extension is accommodated by subaerial faults outside of the lake basin. Consideration of any of these factors will tend to increase this age estimate; more age constraints on older sediments, and more data on subsidence west of Idjwi Island is needed to constrain this error.

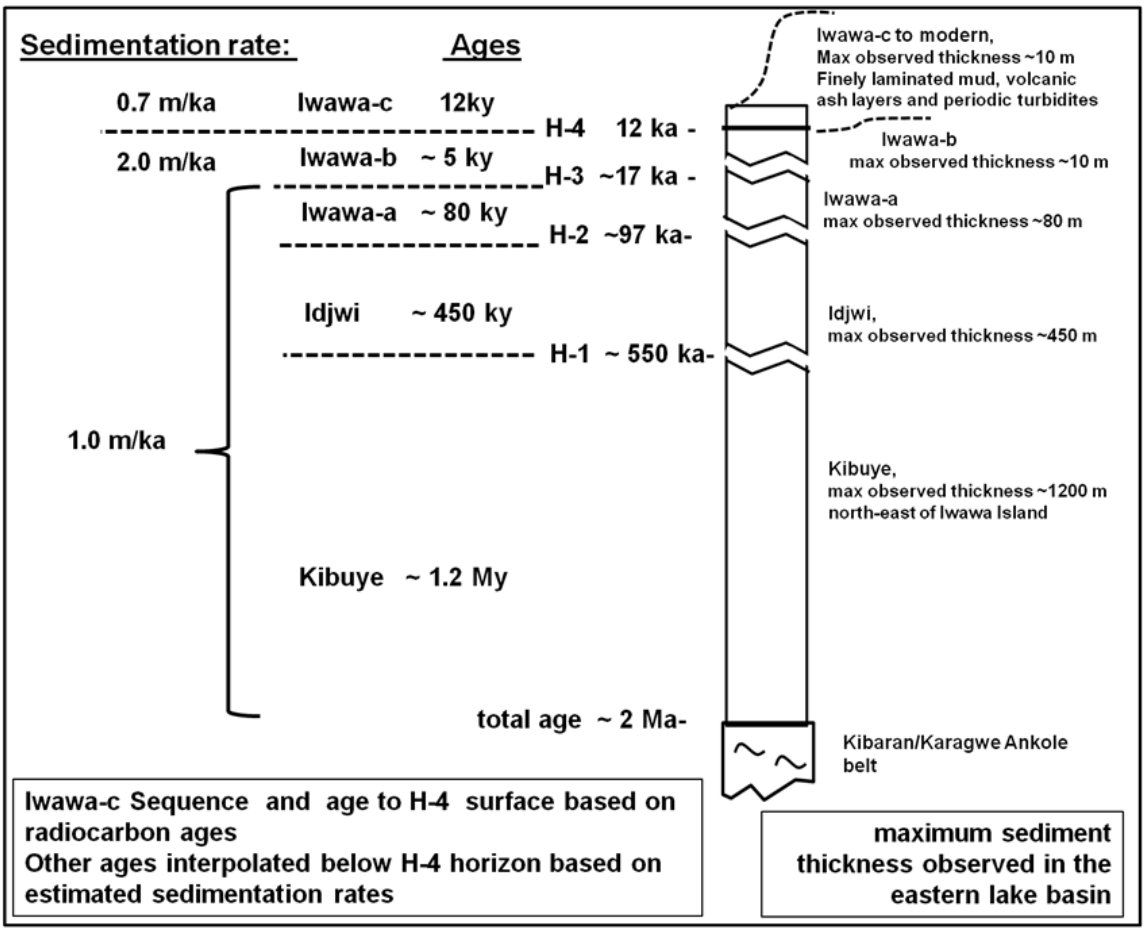

Figure 30. Estimated sedimentary sequence ages, and age to each surface. Horizons H-1, H-2, and H-3 represent desiccation surfaces which are interpreted to correlate to dry climate periods. Depositional surface H-4 is near a rapid lake transgression and shift to a pluvial climate period. Iwawa-c and H-4 age is extrapolated from radiocarbon ages. Other sequence ages are calculated from the maximum sediment thickness observed divided by the estimated sedimentation rates of 2 m/ka for the Iwawa-b Sequence and 1 m/ka for the Iwawa-c, Idjwi, and Kibuye Sequences.

Studying the basin structure and paleolimnology of Lake Kivu will help understand the lakes influence on much larger Lake Tanganyika, and will enhance the understanding of geo-hazards in the Lake Kivu catchment. In order to better constrain basin history, future work must include new seismic reflection data from DRC territorial waters, and deeper sediment cores that can penetrate into earlier lake stage sediments. Onshore drilling in the Virunga Province can also determine volcanic accretion rates to determine the cause of historic lake transgressions, and map

the lake's earlier northern extension. These data could determine the location of the oldest sediments, the timing and direction of rifting, and any possible resources within the lake sediments. Samples from deeper cores will better constrain sediment deposition rates of earlier lake stages and events to enable more accurate regional stratigraphic correlations. Lake Kivu might provide the most precise climate record in the region because it is located at the high point of the western rift and its sedimentary record is not overprinted by inflow from other lake basins.

Conclusions:

1: The eastern basin of Lake Kivu is a half-graben formed by sub-parallel north-striking normal faults, which dip to the east, and which are synthetic to the main border fault system on the western shore of the lake. Most eastern basin subsidence is accommodated by two faults along the eastern sides of Idjwi and Iwawa Islands. A northeast-striking oblique slip transfer fault south of Iwawa Island accommodates strain between these faults. Northeast-striking faults in the north of the basin show little recent activity and may be remnant from an episode of earlier, NW-SE extension. Oblique strike slip accommodated by earlier northeast striking normal faults may account for the irregular shape of the Kivu Basin.

2: Eastern basin extension is measured to be at least ~2.1 km, and overall extension across the Kivu rift is interpolated to be at least ~5 km.

3: Sediments are at least 1500 m thick in the Rwandan territorial waters of the East Kivu Graben and may be thicker to the west in the DRC.

4: Eastern basin sedimentation was interrupted by at least three different truncation surfaces which are interpreted to represent extended periods of aridity. The most recent is estimated to have ended ~17 ka and may correlate to the LGM. The next oldest erosional surface is estimated to have ended ~97 ka and is the most extensive unconformity in the record. This event may correlate to the regional megadrought reported to have occurred between ~135-70 ka. The third and oldest desiccation event ended ~550 ka.

5: The minimum age estimate of the oldest eastern basin sediments observed is ~2 Ma calculated from estimated sedimentation rates for each lake period, or ~1 Ma calculated from extension observed within the basin divided by the estimated extension rate.

6: Before ~17 ka the lake stood at a maximum level of ~310 m below its current surface level, and this is interpreted as the approximate height of a northern basinal spill point. After ~17 ka, the lake transgressed from near desiccation, to a level ~370 m below the current lake stand. The lake remained near this level, underfilling the basin for ~5 ky. Sometime before, or during this lake lowstand, the Virunga Volcanic Complex expanded to obstruct the northern outlet of the lake. At ~12 ka, wetter climate conditions raised the lake level by ~400 m to spill out of the Bukavu Basin to the south. This ~400 m lake transgression occurred over an interval of ~100 years.

References:

Bally, A.W., 1988, Atlas of Seismic Stratigraphy: AAPG Studies in Geology, n. 27, v. 2.

Beadle, L.C., 1981, The Inland Waters of Tropical Africa, an Introduction to Tropical Limnology, second edition: Longman Group Ltd., London. Ch. 15: Volcanic-barrier lakes: Lake Kivu, p. 267-275.

Bhattarai, S., Ross, K.A., Schmid, M., Anselmetti, F.S., and Bürgmann, H., 2012, Local conditions structure unique Archaeal communities in the anoxic sediments of meromictic Lake Kivu: Microbial Ecology, v. 64, n. 2, p. 291-300.

Brooks, J.L., 1950, Speciation in Ancient Lakes: Quarterly of Biology, v. 25, p. 30-60.

Carroll, A.R., and Bohacs, K.M., 1999, Stratigraphic classification of ancient lakes: Balancing tectonic and climatic controls: Geology, v. 27, n. 2, p. 99-102.

Cohen, A.S., Stone, J.R., Beuning, K.R., Park, L.E., Reinthal, P.N., Dettman, D., Scholz, C.A., Johnson, T.J., King, J.W., Talbot, M.R., Brown, E.T., Ivory, S.J., 2007, Ecological consequences of early Late Pleistocene megadroughts in tropical Africa: Proceedings of the National Academy of Sciences, v. 104, n. 42, p. 16422-16427.

Crowe, S.A., O'Neill, A.H., Katsev, S., Hehanussa, P., Haffner, G.D., Sundby, B., Mucci, A., and Fowle, D.A., 2008, The biogeochemistry of tropical lakes: A case study from Lake Matano, Indonesia: Limnology and Oceanography, v. 53, n. 1, p. 319-331.

Degens, E.T., von Herzen, R.P., Wong, H-K., Deuser, W.G., and Jannasch, H.W., 1973, Lake Kivu: Structure, Chemistry and Biology of an East African Rift Lake: Geological Research, v. 61, p. 245-277.

deMenocal, P., Ortiz, J., Guilderson, T., Adkins, J., Sarnthein, M., Baker, L., and Yarusinsky, M., 2000, Abrupt onset and termination of the African Humid Period: rapid climate responses to gradual insolation forcing: Quaternary Science Reviews, v. 19, n. 1, p. 347-361.

d'Oreye, N., González, P.J., Shuler, A., Oth, A., Bagalwa, L., Ekström, G., Kavotha, D., Kervyn, F., Lucas, C., Lukaya, F., Osodundu, E., Wauthier, C., and Fernández, J., 2011, Source parameters of the 2008 Bukavu-Cyangugu earthquake estimated from InSAR and teleseismic data: Geophysical Journal International, v. 184, n. 2, p. 934-948.

Danzeblocke, U., Jöris, O., and Weniger, B., 2013, CalPal-2007^{online}. http://calpal-online.de. Accessed 21 June, 2013.

Ebinger, C.J., 1989a, Tectonic development of the western branch of the East African Rift System: Geological Society of America Bulletin, v. 101, n.7, p. 885-903.

Ebinger, C.J., 1989b, Geometric and kinematic development of border faults and accommodation zones, Kivu-Rusizi rift, Africa: Tectonics, v. 8 n. 1, p. 117-133.

Ebinger, C.J., and Furman, T., 2002, Geodynamical setting of the Virunga volcanic province, East Africa: Acta Vulcanologica, v. 14, n. 1/2, p. 9.

Ebinger, C.J., and Sleep, N.H., 1998, Cenozoic magmatism throughout east Africa resulting from impact of a single plume: Nature, v. 395, n. 6704, p. 788-791.

Environmental and Social Impact Assessment (EISA) Summary, Kivuwatt Power Project, 2010, Government of Rwanda project number P-RW-FGO-001.

Felton, A.A., Russell, J.M., Cohen, A.S., Baker, M.E., Chesley, J.T., Lezzar, K.E., McGlue, J.S., Pigati, J.Q., Stager, J.C., and Tiercelin, J.J., 2007, Paleolimnological evidence for the onset and termination of glacial aridity from Lake Tanganyika, Tropical East Africa: Paleogeography, Paleoclimatology, Paleoecology, v. 252, n. 3, p. 405-423.

Haberyan, K.A., Hecky, R.E., 1987, The Late Pleistocene and Holocene Stratigraphy and Paleolimnology of Lakes Kivu and Tanganyika: Paleogeography, Paleoclimatology, Paleoecology, v. 61, p.169-197.

Halfman, J.D., and Johnson, T.C., 1988, High-resolution record of cyclic climatic change during the past 4 ka from Lake Turkana, Kenya: Geology, v. 16, n. 6, p. 496-500.

Hecky, R.E., and Degens, E.T., 1973, Late Pleistocene-Holocene chemical stratigraphy and paleolimnology of the Rift Valley lakes of Central Africa: Woods Hole Oceanographic Institution, Tech. Report No. 73-28, 93 p.

Johnson, T.C., 1996, Sedimentary processes and signals of past climatic change in the large lakes of the East African Rift Valley: The Limnology, Climatology and Paleoclimatology of the East African Lakes, Gordon and Breach, Amsterdam, p. 367-412.

Johnson, T.C., Scholz, C.A., Talbot, M.R., Kelts, K., Ricketts, R.D., Ngobi, G., Beuning, K., Ssemmanda, I., and McGill, J.W., 1996, Late Pleistocene desiccation of Lake Victoria and rapid evolution of cichlid fishes: Science, v. 273, n. 5278, p. 1091-1093.

Kampunzu, A.B., Bonhomme, M.G., and Kanika, M., 1998, Geochronology of volcanic rocks and evolution of the Cenozoic Western Branch of the East African Rift System: Journal of African Earth Sciences, v. 26, n. 3, p. 441-461.

Kempe, S., and Degens, E.T., 1985, An early soda ocean?: Chemical Geology, v. 53, n. 1, pp. 95-108.

Kling, G.W., Clark, M.A., Compton, H.R., Devine, J.D., Evans, W.C., Humphrey, A.M., Koenigsberg, E.J., Lockwood, J.P., Tuttle, M.L., and Wagner, G.N., 1987, The 1986 Lake Nyos Gas Disaster in Cameroon, West Africa: Science, v. 236, n. 4798, p. 169-175.

Moernaut, J., Verschuren, D., Charlet, F., Kristen, I., Fagot, M., and De Batist, M., 2010, The seismic-stratigraphic record of lake-level fluctuations in Lake Challa: Hydrological stability and change in equatorial East Africa over the last 140kyr: Earth and Planetary Science Letters, v. 290, n.1, p. 214-223.

Muvundja, F.A., Pasche, N., Bugenyi, F.W.B., Isumbisho, M., Müller, B., Namugize, J.N., Rinta, P., Schmid, M., Stierli, R., and Wüest, A., 2009, Balancing nutrient inputs to Lake Kivu: Journal of Great Lakes Research, v. 35, n. 3, p. 406-418.

Nyblade, A.A., and Brazier, R.A., 2002, Precambrian lithospheric controls on the development of the East African rift system: Geology, v. 30, n. 8, p. 755-758.

Olson, E.A., Broecker, W.S., 1959, Lamont Natural Radiocarbon Measurements: American Journal of Science, v. 257, p. 1-28.

Pasteels, P., Villeneuve, M., De Paepe, P., and Klerkx, J., 1989, Timing of the volcanism of the southern Kivu province: implications for the evolution of the western branch of the East African Rift system: Earth and Planetary Science Letters, v. 94, n. 3, p. 353-363.

Roberts, E.M., Stevens, N.J., O'Connor, P.M., Dirks, P.H.G.M., Gottfried, M.D., Clyde, W.C., Armstrong, R.A., Kemp, A I.S., and Hemming, S., 2012, Initiation of the western branch of the East African Rift coeval with the eastern branch: Nature Geoscience, v. 5, n.4, p. 289-294.

Russell, J.M., and Johnson, T C., 2005, A high-resolution geochemical record from Lake Edward, Uganda Congo and the timing and causes of tropical African drought during the late Holocene: Quaternary Science Reviews, v. 24, n. 12, p. 1375-1389.

Schmid, M., Halbwachs, M., Wehrli, B., and Wuest, A., 2005, Weak mixing in Lake Kivu: New Insights Indicate Increasing Risk of Uncontrolled Gas Eruption: G^3, AGU, and Geochemical Research Letter, vol. 6, n. 7

Scholz, C.A., and Rosendahl, B.R., 1988, Low lake stands in Lakes Malawi and Tanganyika, East Africa, delineated with multifold seismic data: Science, New Series, v. 240, n. 4859, p. 1645-1648.

Scholz, C.A., 2002, Applications of seismic sequence stratigraphy in lacustrine basins: Tracking environmental change using lake sediments, p. 7-22, Springer, Netherlands.

Scholz, C.A., King, J. ., Ellis, G.S., Swart, P.K., Stager, J.C., and Colman, S.M., 2003, Paleolimnology of Lake Tanganyika, East Africa, over the past 100 kyr: Journal of Paleolimnology, v. 30, n. 2, p.139-150.

Scholz, C.A., Johnson, T.C., Cohen, A. ., King, J.W., Peck, J.A., Overpeck, J.T., Talbot, M.R., Brown, E.T., Kalindekafe, L., Amoako, P.Y.O., Lyons, R.P., Shanahan, T.M., Castañeda, I.S., Heil, C. W., Forman, S.L., McHargue, L.R., Beuning, K.R., Gomez, J., Pierson, J., 2007, East African megadroughts between 135 and 75 thousand years ago and bearing on early-modern human origins: Proceedings of the National Academy of Sciences, v. 104, n. 42, p. 16416-16421.

Smets, B., Wauthier, C., and d'Oreye, N., 2010, A new map of the lava flow field of Nyamulagira (DR Congo) from satellite imagery: Journal of African Earth Sciences, v. 58, n. 5, p. 778-786.

Spigel, R.H., and Coulter, G.W., 1996, Comparison of hydrology and physical limnology of the East African great lakes: Tanganyika, Malawi, Victoria, Kivu and Turkana (with reference to some North American Great Lakes): The limnology, climatology and paleoclimatology of the East African lakes, p. 103-139.

Stager, J.C., and Johnson, T.C., 2008, The late Pleistocene desiccation of Lake Victoria and the origin of its endemic biota: Hydrobiologia, v. 596, n. 1, p. 5-16.

Stamps, D.S., Calais, E., Saria, E., Hartnady, C., Nocquet, J.M., Ebinger, C.J., and Fernandes, R.M., 2008, A kinematic model for the East African Rift: Geophysical research letters, v. 35, L05304.

Stoffers, P., and Hecky, R.E., 1978, Late Pleistocene-Holocene evolution of the Kivu-Tanganyika Basin: International Association of Sedimentology, special publication, v.2, p. 43-55.

Tiercelin, J.J., and Lezzar, K.E., 2004, A 300 million years history of rift lakes in Central and East Africa: an updated broad review, p. 3-60,: In Odada, E.O., and Olago, D.O. (eds.), The East African Great Lakes: Limnology, Palaeolimnology and Biodiversity, Springer, Netherlands, 588 p.

Tietze, K., 2000, Lake Kivu Gas Development and Promotion-related Issues: Safe and Environmentally Sound Exploration, PDT report no. 520002: Republic of Rwanda, Ministry of Energy, Water and Natural Resources, Unit for the Promotion and Exploitation of Lake Kivu Gas, Kigali, 110 p.

Tietze, K., Geyh, M., Müller, H., Schröder, L., Stahl, W., and Wehner, H., 1980, The genesis of the methane in Lake Kivu (Central Africa): Geologische Rundschau, v. 69, n. 2, p. 452-472.

Wilkinson, B.H., Pope, B.N., and Owen, R.M., 1980, Nearshore ooid formation in a modern temperate region marl lake: The Journal of Geology, v. 88, n. 6, p. 697-704.

Wong, H.K., and von Herzen, R.P., 1974, A Geophysical Study of Lake Kivu, East Africa: Geophysical Journal of the Royal Astronomical Society, v. 37, n. 3, pp. 371-389.

Zal, H.J., 2013, Mapping active faults in the Kivu Rift Basins from digital elevation models calibrated by seismic and field data [Senior Thesis]: University of Rochester, Rochester, NY.

Vita:

D. A. Wood, C. A. Scholz, X. Zhang, 2013, Basin history of the eastern graben of Lake Kivu from marine seismic reflection data: Active Volcanic and Continental Rifting annual meeting (AVCoR2013), Gisenyi, Rwanda, poster presentation.

D.A. Wood, C. A. Scholz, Interpretation of marine seismic reflection data of the eastern graben of Lake Kivu, Rwanda: Geological Society of America 2013 meeting, Denver, CO.

L.J. Poppe, K.Y. McMullen, K.Y. Ackerman, M.R. Guberski, and **D.A. Wood**, Sea-floor character and sedimentary processes offshore of the Connecticut River, Northern Long Island Sound: Geological Society of America 2013 meeting, Denver, CO., poster presentation.

C.A. Scholz, X. Zhang, **D.A. Wood**, D. Mburu, 2012, Extension and basin evolution of the East Kivu Graben, Rwanda, East African Rift: results of new multichannel seismic reflection imaging: American Geophysical Union fall meeting.

L.J. Poppe, K.Y. McMullen, S.D. Ackerman, M.R. Guberski, and **D.A. Wood,** 2013, Sea-floor character and geology off the entrance to the Connecticut River, northeastern Long Island Sound: U.S. Geological Survey Open-File Report 2012–1103.

D.A. Wood, C.A. Scholz, 2012, Evolution of a magmatically active extensional basin: new multichannel seismic data from Lake Kivu, Rwanda, Syracuse University's Lacustrine and Rift Basin Research sponsors' meeting, November, 2012, Houston, Texas, (oral presentation).

D.A. Wood, C.A. Scholz, 2011, Rifting and magnetism around South Island, Lake Turkana, Kenya using high resolution, multi-beam SONAR, Syracuse University's Lacustrine and Rift Basin Research sponsors' meeting, September, 2011, Woodlands, Texas, (oral presentation).

K.Y. McMullen, L.J. Poppe, S.D. Ackarman, D.S. Blackwood, J.D. Schaer, M.A. Nadeau, and **D.A. Wood**, 2011, Surficial Geology of the Sea Floor in Central Rhode Island Sound Southeast of Point Judith, Rhode Island, USGS Open-file Report 2011-1005.

K.Y. McMullen, L.J. Poppe, W.W. Dandorth, D.S. Blackwood, J.D. Schaer, M.R. Guberski, **D.A. Wood**, and E.F. Doran, 2010, Surficial Gelolgy of the Sea Floor in Long Island Sound Offshore of Orient Point, New York, USGS Open-file Report 2010-1100.